Published in final edited form as:

Physiol Rev. 2010 October ; 90(4): 1547–1581. doi:10.1152/physrev.00013.2010.

Intrinsically Photosensitive Retinal Ganglion Cells

MICHAEL TRI HOANG DO and **KING-WAI YAU**

Solomon H. Snyder Department of Neuroscience and Center for Sensory Biology, Johns Hopkins University School of Medicine, Baltimore, Maryland

Abstract

Life on earth is subject to alternating cycles of day and night imposed by the rotation of the earth. Consequently, living things have evolved photodetective systems to synchronize their physiology and behavior with the external light-dark cycle. This form of photodetection is unlike the familiar "image vision," in that the basic information is light or darkness over time, independent of spatial patterns. "Nonimage" vision is probably far more ancient than image vision and is widespread in living species. For mammals, it has long been assumed that the photoreceptors for nonimage vision are also the textbook rods and cones. However, recent years have witnessed the discovery of a small population of retinal ganglion cells in the mammalian eye that express a unique visual pigment called melanopsin. These ganglion cells are intrinsically photosensitive and drive a variety of nonimage visual functions. In addition to being photoreceptors themselves, they also constitute the major conduit for rod and cone signals to the brain for nonimage visual functions such as circadian photoentrainment and the pupillary light reflex. Here we review what is known about these novel mammalian photoreceptors.

I. INTRODUCTION

It was long axiomatic that rods and cones are the only mammalian photoreceptors. Light hyperpolarizes these neurons, and the light signals propagate through the retinal circuitry to modulate spike firing in the retinal ganglion cells (RGCs). The RGCs send the light information to the brain via their axons, which constitute the optic nerve. The most prominent targets of RGC axons are the dorsal lateral geniculate nucleus (dLGN), the way station for light information en route to visual cortex, and other regions involved in conventional image vision. In addition, some RGC axons transmit light information to brain centers for "nonimage" visual functions such as circadian photoentrainment.

The original belief was that all light signals for image and nonimage vision alike began with the rods and cones. In retrospect, some clues against this belief had already appeared decades ago, although convincing evidence has emerged only within the past 10 years. A suggestion that rod and cone photoreceptors do not account for the spectral sensitivity of the

Addresses for reprint requests and other correspondence: M. Do or K.-W. Yau, Rm. 905A, Preclinical Teaching Bldg., Johns Hopkins University School of Medicine, 725 North Wolfe St., Baltimore, MD 21205, michaeltri.do@childrens.harvard.edu and kyau@jhmi.edu.

DISCLOSURES

No conflicts of interest, financial or otherwise, are declared by the authors.

pupillary light reflex can be found as early as 1923 (see Ref. 126). In 1980, it was reported that light regulated dopamine levels in rat retinas even after profound degeneration of the rods and cones (129). Ten years later, the evidence became more urgent when mice with degenerated rods and cones (homozygous for *retinal degeneration*, *rd/rd*) were found to shift their circadian rhythms according to the external light-dark cycle, rather like wild-type mice (51, 158) but with a spectral sensitivity unlike that of rods and cones (230). Similar observations were made in humans; namely, light remained effective in suppressing pineal melatonin secretion and entraining the circadian clock in some people who were blind from severe loss of rods and cones, without impinging on conscious perception (34, but see Ref. 232) (Fig. 1, *A* and *B*). At the same time, newborn mice, which had yet to develop rods and cones, were found to show photic activation of the suprachiasmatic nucleus (SCN), the master circadian pacemaker, suggesting that the retina was already feeding light signals into the retinohypothalamic tract (RHT) (222). Even circadian photoentrainment in wild-type animals exhibited some features that were considered unusual for rod- and cone-based signaling, namely, low sensitivity to light and integration of light over long durations (137, 189).

In the above early studies, it could not be completely ruled out that a small number of rods and cones, either surviving retinal degeneration or somehow appearing ahead of developmental schedule, were sufficient for nonimage vision. Cones were especially troublesome because they are not directly affected by the *rd* mutation, but die secondary to the loss of rods. Nonetheless, rodless/coneless mice obtained from crossing rod-degenerated mice (*rd/rd* as above, or *rdta,* in which rods are ablated by targeted expression of diphtheria toxin) with a cone-ablated line (*cl*, by targeted expression of diphtheria toxin in cones) still responded to light with a phase shift of the circadian rhythm (52) and a suppression of pineal melatonin production (115) (Fig. 1, *C–E*). Moreover, these mice displayed a pupillary light reflex with a spectral sensitivity suggestive of a single, vitamin A-based photopigment most sensitive to ~480-nm light (113). Rods and cones alone would have produced a much different spectral-sensitivity profile. These nonimage visual functions in rodless/coneless mice still required, however, illumination of the eyes (52, 115). Hence, there indeed appeared to be a hitherto-undiscovered ocular photoreceptor, one most sensitive to turquoise light.

In parallel, a molecular search was underway for new photopigments. Screening the photosensitive dermal melanophores of *Xenopus laevis*, Provencio et al. (155) discovered an opsin that they named melanopsin (Fig. 2*A*). Soon after its discovery, melanopsin was localized to a small subset (~1–2%) of RGCs in the rodent eye (Fig. 2*B*) (62, 88, 156, 157). These melanopsin-expressing RGCs project through the RHT to the SCN, and to a variety of other brain regions serving nonimage vision (Fig. 3) (63, 75, 87, 88).

Berson et al. (17) also showed in breakthrough work that RGCs projecting to the SCN were bona fide photoreceptors. By injecting a vital fluorescent marker into the rat SCN, they succeeded in retrograde-labeling these rare neurons for patch-clamp recording and observed a light response even after pharmacologically blocking all signals from the rod and cone pathways (Fig. 2*C*). This intrinsic light response was a depolarization that drove action potentials, the same polarity as that in most invertebrate photoreceptors but opposite to the

hyperpolarizing light response in rods and cones (17). Concurrently, these intrinsically photosensitive RGCs (ipRGCs) and melanopsin-expressing RGCs were shown to be one and the same (88). Melanopsin-expressing RGCs have since been found in every mammalian species examined, including subterranean mole rat (78), rabbit (79, 94), cat (180), and primate (35, 99) including human (35) (Fig. 4). The melanopsin-expressing RGCs are also distinguished from conventional RGCs by their expression of pituitary adenylyl cyclase-activating protein (PACAP), a peptide neuromodulator that may play an important role in nonimage vision (77, 79). Many brain targets of the ipRGCs express PACAP receptors, and animals with impaired PACAP signaling are defective in circadian photoentrainment, among other functions (14, 31, 81, 84).

In adult mammals, melanopsin appears to be expressed in no other cell type besides ipRGCs (but see Refs. 37, 55, 147), and all ipRGCs appear to express melanopsin. Therefore, we will refer to these cells as melanopsin cells, melanopsin RGCs, or ipRGCs.

There has been a surge of research in the past decade on the physiological importance of ipRGCs and the mechanisms underlying their photosensitivity. We review here fairly comprehensively what has been found. For other perspectives and emphases, we refer the reader to several recent, briefer reviews (3, 15, 72, 73, 106, 136).

II. INTRINSICALLY PHOTOSENSITIVE RETINAL GANGLION CELLS AS ENCODERS OF LUMINANCE

A dozen or more types of RGCs have been identified in the mammalian retina based on form and/or function (59, 121). IpRGCs have been described as straightforward encoders of ambient light (17, 35), equivalent to the “luminance units” discovered by Barlow and Levick (6) in the cat. The latter units are distinguished from other RGCs by their rarity (<1% of the units recorded, comprising just 3 units in the sample by Barlow and Levick), response sluggishness, sustained firing, and a relatively straightforward relationship between steady-state spike frequency and light intensity (6). Upon an increment in light intensity, these units displayed a transient bout of high-frequency firing that relaxed to a steady plateau. In response to a decrement in light intensity, spiking simply decreased to a lower steady rate (6). The steady spike rate was stereotypic for a given intensity, regardless of light increment or decrement, and increased monotonically with increasing light intensity over several log units of light intensity (6). This property is different from conventional RGCs, which can show complex relations between spike rate and light intensity.

A strict identification of ipRGCs as Barlow and Levick’s luminance units is, however, presently not possible for two main reasons: *1*) the spiking of ipRGCs in response to increments and decrements of light has not been reported (stimuli of different intensities have always been preceded with an intervening period in darkness), and *2*) ipRGC spiking has not always been quantified in ways that permit direct comparison with the early work. That said, ipRGCs do bear a strong resemblance to the luminance units. Thus, in response to a step of light, ipRGCs exhibit a transient peak in spike rate that relaxes to a steady plateau (Figs. 2*C* and 8) (17, 35, 205). This is true regardless of whether the spiking is driven by the intrinsic photocurrent alone or together with synaptic input from the rod and cone pathways

(35, 228). Spiking during the steady plateau is sustained for as long as has been measured (up to tens of minutes) (17, 35, 205, 159). Spiking of ipRGCs is also sluggish, beginning after a long latency for a dim stimulus and persisting for minutes after termination of an intense light stimulus (Fig. 8*A*) (17, 35, 159, 205). Finally, the relation between spiking and stimulus intensity is monotonic over several orders of magnitude (Fig. 2*D*) (35, 205, 219). Like the luminance units, ipRGCs are also rare (~2% of total RGCs in rat and ~1% in mouse; but see below). It is noteworthy that Barlow and Levick actually suggested that the luminance units be further studied by way of the pupil-constriction pathway (6), the first station (the OPN) of which was demonstrated 40 years later to be none other than a major target of the ipRGCs (Fig. 3*E*) (35, 63, 87, 88).

III. DIVERSITY OF INTRINSICALLY PHOTOSENSITIVE RETINAL GANGLION CELLS AND THEIR PROJECTIONS

A. Morphology and Diversity of ipRGCs

IpRGCs are distinguished from conventional RGCs by their expression of melanopsin, which is present on both the soma and the dendrites at comparable densities (11, 17, 39, 88, 157). The dendrites of ipRGCs are sparse, irregular, far-ranging, and marked by prominent varicosities. These varicosities appear unremarkable except for an enrichment of mitochondria and an obvious increase in surface area (11). Apart from being photosensitive, the dendrites of ipRGCs receive synapses from bipolar and amacrine cells (11, 43, 94, 142, 208) (and also form synapses onto other retinal neurons; see below). The axons of the ipRGCs also express melanopsin, but only up to the optic disc and not beyond (88). The low conduction velocity of RHT-tract fibers together with anatomical evidence suggests that ipRGC axons, unlike those of conventional RGCs, are unmyelinated (24, 69, 102, 141). In primates, the ipRGCs bear broadly similar features except that these are, unlike in rodents, the largest RGCs known. Whether primate ipRGC axons are myelinated is not clear.

While ipRGCs generally appear to share the above-described characteristics, subclasses have been distinguished based on morphology, absolute photosensitivity, and other intrinsic electrophysiological properties (Figs. 3 and 4). We first discuss these subtypes in the rodent, where they have been studied most, then say a few words about them in primates. These ipRGC subtypes also differ with respect to their retinal circuitry and supposedly their projections to the brain, which are discussed in later sections.

Strictly speaking, the above-reported features of ipRGCs belong only to the first-discovered subclass of ipRGCs, the so-called “M1” cells. Rodent M1 cells have somata of ~15 μm diameter, most of which are located in the ganglion cell layer (GCL), although some are displaced to the inner nuclear layer (INL). Even though the M1 cells constitute just ~1% (~700–900 overall) of the total mouse RGC population, their ~300-μm-diameter dendritic fields overlap to cover the entire retina in what has been termed a “photoreceptive net” (Figs. 2*B* and 4*B*) (16, 88, 157). The most obvious characteristic that distinguishes between ipRGC subtypes is where their dendrites stratify in the inner plexiform layer (IPL). Those of M1 cells stratify at the outermost margin of the IPL, at the border with the INL (Fig. 4). This is within the “OFF-sublamina” of the IPL, where OFF-bipolar cells (which depolarize in

response to light decrement) arborize their axon terminals. In spite of this, M1 cells actually receive synaptic input from ON-bipolar cells (which depolarize in response to light increment; see below and Refs. 43, 94). Among the ipRGC subclasses, the M1 cells have noticeably higher melanopsin immunoreactivity (9, 86, 87, 173). Consistent with a correspondingly higher probability of photon capture due to the presumably higher melanopsin density (39), M1 cells show the highest intrinsic photosensitivity of the ipRGC subclasses; they also produce the largest maximum intrinsic photocurrent (173). Curiously, despite their large photocurrent, the M1 cells are prone to depolarization block, being able to fire spikes only at relatively low rates (Fig. 5*D*) (173, 228). The photocurrent itself is large enough to drive the cells into this depolarization block (173, 228).

Compared with M1 cells, rodent M2 cells have larger (~20 μm) somata and more regular-branching dendrites that cover a larger area (~400 μm) (Fig. 4*A*) (9, 16, 87, 173, 208). M2 cells are as numerous as M1 cells (9, 16, 87, 208) and cover the entire retina (16). Importantly, the dendrites of the M2 cells stratify on the opposite side of the IPL from the M1 cells, where the ON-sublamina of the IPL borders the GCL (9, 87, 173, 208) (Fig. 4*A*). Thus the M1 and M2 cells are likely to participate in different retinal circuits (see below). M2 cells are 10-fold less intrinsically photosensitive than M1 cells, and they produce a 10-fold smaller maximum photocurrent (173) (Fig. 5, *A* and *B*). At the same time, they can fire action potentials at far higher frequencies than the M1 cells (173) (Fig. 5*D*). Thus synaptic input may be more important for driving the M2 cells over their full dynamic range than it is for driving the M1 cells (see below and Ref. 99).

The final reported subtype of rodent ipRGCs comprises the M3 cells, which stratify their dendrites in both the ON-and OFF-sublaminae of the IPL (Fig. 4*A*) (16, 174, 208). M3 cells are ~10% of the ipRGCs (16; but see Refs. 174 and 208) and, because they apparently do not cover the retina, may not constitute a true cell type (16). Many of their properties, including their sensitivity to light and synaptic inputs, have yet to be determined. Preliminary evidence suggests the existence of additional ipRGC subtypes (16, 86).

Heterogeneity in the ipRGC population was also suggested early on by imaging experiments. In the GCL of rodless/coneless retinas, there are cells that generate sustained, transient, or repetitive Ca^{2+} signals upon illumination (176). How these imaged subtypes map onto the ipRGC subtypes described above is unclear, as the morphologies of the imaged subtypes are undefined, and the relationship of their Ca^{2+} dynamics to other electrophysiological properties is unknown. Another early demonstration of ipRGC heterogeneity was based on multielectrode-array recordings in rodless/coneless mice, which identified two physiological subclasses in the adult based on sensitivity and spike latency. Despite the lack of morphological information, the differential sensitivities of these cells suggest that they are the M1 and M2 subtypes described above (Fig. 5, *B* and *C*) (205).

In the macaque-monkey retina, there are ~3,000 ipRGCs, constituting 0.2% of the total RGC population (35). The ipRGC dendrites form a highly overlapping mesh that covers the entire retina except for the fovea, which the cells encircle but do not enter (Fig. 4*B*) (35). The dendritic field diameters of the ipRGCs are the largest known of all primate RGCs, exceeding 1 mm in the peripheral retina (35). The somata are also giant, approaching ~50

μm in diameter. These ipRGCs appear to be also principally monostratified, with one subtype stratifying in the OFF-sublamina of the IPL and the other stratifying in the ON-sublamina (Fig. 4*C*); some are bistratified, however (35, 36). The situation in the marmoset, a new-world monkey, is largely the same (99). It seems reasonable to conjecture that the OFF-, ON-, and bistratified cells of primates correspond to the M1, M2, and M3 cells of rodents, respectively.

B. Brain Regions Innervated by ipRGCs

The ipRGCs send their axons to well over a dozen regions in the brain (Fig. 3 and Table 1). Most notable among these are the SCN (the master circadian clock), the intergeniculate leaflet (IGL, a center for circadian entrainment), the olivary pretectal nucleus (OPN, a control center for the pupillary light reflex), the ventral sub-paraventricular zone (vSPZ, implicated in "negative masking," or acute arrest of locomotor activity by light in nocturnal animals), and the ventrolateral preoptic nucleus (VLPO, a control center for sleep) (63, 75, 87, 88). Other projections that are more enigmatic in function include those to the lateral habenula and amygdala (87). Interestingly, the axon of a single melanopsin cell in hamster can branch and innervate at least two different brain regions, suggesting some common information being transmitted for different behaviors (130).

The majority of the above ipRGC targets are also innervated by conventional RGCs, with the proportions varying across brain regions (Table 1). These proportions also vary across species. For instance, virtually all retinal innervation of the SCN in mouse is from ipRGCs (9, 70, 87), whereas in the hamster, the ipRGCs constitute 80–90% (185). Whether these varying proportions of inputs from ipRGCs and conventional RGCs correspond to some differences in nonimage vision across species is unclear. The dLGN apparently receives very few ipRGC fibers in mouse and rat (63, 75, 87), but possibly many in the macaque (35). However, some of these apparent variations across species may potentially be due simply to the preferential study of the M1 ipRGCs in rodents. In the *Opn4*$^{-/-}$ *tau-lacZ*$^{+/+}$ mouse used for the axonal-projection study, the tau-β-galactosidase activity coded by *tau-LacZ* was reportedly found only in the M1 subtype, probably because of a higher level of melanopsin expression and thus the cell marker (9, 87). Likewise, the axons of ipRGCs have been traced by preferential labeling with a low-titer injection of recombinant adeno-associated virus carrying GFP (rAAV-GFP) (63), which apparently also selects for the M1 cells (9, 63). Recent unpublished work, however, suggests that the other ipRGC subtypes may have quite different projection targets such as the dLGN (22, 86).

IV. FUNCTIONS OF THE MELANOPSIN SYSTEM

A. Role of Photosignaling by Melanopsin

The ipRGCs of melanopsin-null (*opn4*$^{-/-}$) mice appear to develop with normal morphology, axonal projections, and cell number but lack intrinsic photosensitivity entirely (116). These animals show some functional impairment, attesting to the importance of light-sensing by melanopsin in driving behavior (116, 133, 145, 166). Mice have also been generated that lack signaling from rods and cones. Rod function was disabled by knockout of rod transducin (*gnat1*$^{-/-}$) (27) or rhodopsin (*rho*$^{-/-}$) (109), or rods were killed altogether by

induced degeneration (*rd/rd*) or targeted expression of diphtheria toxin (*rdta*) (125); cone function was disrupted by the knockout of a critical subunit of the cone CNG channel (*cnga3*$^{-/-}$) (19) mediating phototransduction, or cones were killed by targeted expression of diphtheria toxin (*cl*) (186). Here we refer to mice resulting from the various crossings of these genotypes as "rodless/coneless" mice, although in some cases they were, strictly speaking, rod/cone-functionless mice. Even in the absence of signaling from rods and cones, ipRGCs are able to drive a variety of behaviors, some with a surprising degree of completeness.

1. Pupillary light reflex—The pupillary light reflex (PLR) serves image vision by reducing the saturation of rod and cone photoreceptors by light, increasing depth of field, and improving resolution. Because of its speed, the PLR is also the most readily quantifiable behavior driven by the ipRGCs and, in fact, was instrumental in characterizing non-rod/non-cone vision prior to the discovery of the ipRGCs themselves (113). In the wild-type mouse, the PLR reaches its maximum constriction over ~6 log units of increasing light intensity. The PLR of *opn4*$^{-/-}$ mice is fairly similar to wild-type until reaching ~80% of maximum constriction, at which point the pupil does not constrict further. In contrast, the PLR of rodless/coneless mice begins only in brighter light, but is capable of reaching the same maximal constriction as wild-type at a similar light intensity (7, 116, 144, 181). These studies indicate that the intrinsic photosensitivity of ipRGCs begins driving the PLR only in relatively bright light but can take it to completion (116). Interestingly, *opn4*$^{-/-}$ mice are capable of holding their PLR only for tens of seconds, after which the pupil dilates again (236). Thus melanopsin phototransduction is also important for sustained pupil constriction for long durations, perhaps to compensate for light adaptation in the rods and cones.

The action spectrum of the PLR in rodless/coneless mice matches that of the ipRGCs (17, 113). Incidentally, humans and dogs with degenerated rods and cones also show a PLR with an elevated threshold and a spectral sensitivity consistent with ipRGC activity (68, 232). Finally, the role of ipRGCs in the normal PLR of monkey and human has likewise been demonstrated (see below and Refs. 56, 126).

2. Circadian photoentrainment—Mice given a pulse of light near the beginning of their rest period will advance their circadian clock (a "positive phase-shift"), whereas light given near the beginning of their active period will delay their clock (a "negative phase-shift") (Fig. 6*A*). The extent of phase-shift increases with brighter light. In melanopsin-null mice, however, the extent of phase-shift reaches a plateau far below the wild-type maximum, implicating the importance of melanopsin signaling to the process (Fig. 6*B*) (145, 166). Qualitatively, the situation is like the PLR, except that, whereas rod/cone signals are able to drive up to 80% of the PLR, their contribution to circadian photoentrainment is far less (no more than 50%, as gleaned from the data of Panda et al., see Ref. 145) (Fig. 6*B*). It should be noted, nonetheless, that melanopsin is not an intrinsic component of the circadian clock itself (145, 166).

Rodless/coneless mice show circadian photoentrainment (7, 52, 89, 144, 181), with an action spectrum that matches that of the ipRGCs (230). Rodless/coneless rats and primates also show circadian photoentrainment (103, 182, 201).

3. Negative masking—When challenged with light, mice and many other nocturnal animals reduce locomotion, a behavior called negative masking (reviewed in Ref. 132). O*pn4*$^{-/-}$ mice show less negative masking than wild type (133, 144). Although wild-type and *opn4*$^{-/-}$ mice both suppress locomotion at a similar threshold light stimulus, the *opn4*$^{-/-}$ mice gradually adapt from negative masking and resume locomotion (Fig. 6*C*) (133). The speed of adaptation is very slow, requiring ~2 h after light onset for relatively dim light (100 lux) and well over an hour even for brighter light (1,650 lux), presumably because rods and cones still play a large role in the behavior in this intensity and time regime (133). Thus the role of melanopsin in negative masking may only become obvious in bright light and over long durations (145).

For wild-type mice, very low light intensities actually cause "positive masking," or an increase in locomotion. Positive masking is thought to reflect the image-forming system helping to guide locomotion. Negative masking, however, develops and dominates in brighter light and is maximal with just ~1 log unit of additional light intensity above that eliciting positive masking (197). Rodless/coneless mice show no positive masking at all, as would be expected from locomotion utilizing the rod/cone-mediated image vision, and negative masking appears at a lower light intensity, reaching the same end point as in wild-type mice (197).

In summary, while only rods and cones drive positive masking at very low light intensities, rods, cones, and ipRGCs all drive negative masking at higher light intensities, and melanopsin signaling is required for maximal and sustained negative masking. In rodless/coneless mice, negative masking has an action spectrum similar to that of the ipRGCs (197). Diurnal animals presumably do not show such behavior.

4. Sleep regulation—Melanopsin also appears important for the regulation of sleep in rodents. A pulse of light given during the dark period will acutely induce sleep in wild-type mice (1, 118, 203). This sleep induction is associated with c-*fos* expression in the ventrolateral preoptic nucleus (203), consistent with the activation of this sleep-promoting brain region (172). A pulse of darkness given during the light period can also induce awakening (1, 203). These effects are lost in the *opn4*$^{-/-}$ mouse (1, 118, 203). Moreover, *opn4*$^{-/-}$ mice show perturbations in sleep homeostasis, with increased bouts of waking and thus loss of sleep (203). The above findings on sleep regulation may apply to diurnal animals like humans, although there would likely be a sign inversion such that light promoted wakefulness. Sign inversions in hypothalamic signaling are not unprecedented; for instance, SCN neurons have elevated spontaneous firing rates during the day in both diurnal and nocturnal animals, although the downstream effects are different (reviewed in Ref. 23).

5. Suppression of pineal melatonin—Melatonin is a neurohormone that is predominantly released from the pineal gland into the brain and bloodstream, reaching its highest level at night and driving a wide variety of physiological responses (reviewed in Ref. 233). Melatonin levels are suppressed by light. Pineal melatonin content can be quantified by either melatonin radioimmunoassay or at the mRNA level for arylalkylamine *N*-acetyltransferase (AA-NAT, the rate-limiting enzyme in melatonin synthesis) (114, 144). At high irradiance, suppression of pineal melatonin is just as complete in rodless/coneless mice

as in wild-type mice (114, 144). Melatonin suppression in humans does have a spectral sensitivity consistent with melanopsin signaling (21, 112, 195).

B. IpRGCs, Rods, and Cones Account for All Ocular Photodetection in Mammals

The discovery of ipRGCs opened up speculation about the potential existence of yet other mammalian photoreceptors waiting to be discovered. Given the existence of quite a few opsinlike proteins of unknown function, this was a realistic possibility (192). Opsins were also not the only candidate photosensors. There was strong speculation about the putative photosensitivity of mammalian cryptochromes, flavenoid-based proteins that form a core component of the mammalian clock and the homolog of which in *Drosophila* is indeed a circadian photoreceptor (179, 196, 206, 207).

At least out of parsimony, however, there is no need for the existence of additional mammalian photoreceptors, or at least those that signal to the brain. "Triple null" mice (*opn4*$^{-/-}$ *gnat1*$^{-/-}$ *cnga3*$^{-/-}$ or *opn4*$^{-/-}$ *rd/rd* genotypes) lacking rod and cone functions, and having no melanopsin showed practically no PLR (Fig. 6*D*), circadian photoentrainment, negative masking, or suppression of AA-NAT even at high light intensities, despite normal retinal morphology and ipRGC projections (89, 144). Thus rods, cones, and ipRGCs together appear to mediate virtually all photodetection for signaling to the brain in mammals. This notion is also supported by the apparent complementarity between rod/cone and ipRGC photodetections for the pupillary light reflex, which over its entire dynamic range in the wild-type mouse can be well accounted for by summing the pupillary light reflexes of rodless/coneless mice and of *opn4*$^{-/-}$ mice (116).

In summary, rods and cones contribute to nonimage visual functions at low light intensities, while melanopsin signaling contributes to these functions at high light intensities. This does not mean, however, that the melanopsin system functions at light intensities well above daily experience. For example, typical room light of a few hundred lux is sufficient for eliciting near-complete negative masking in mouse (145, 197) as well as a half-maximal PLR in rodless/coneless mice (our unpublished observations). It should be noted that "lux" expresses light intensity as a function of human spectral sensitivity and thus has limited meaning for other species. We use lux here because it is more intuitive than the more appropriate radiometric units (photons per unit area and time) (128).

The cryptochromes are probably not involved in photodetection in mammals, unlike in *Drosophila*. For instance, nonimage visual functions are absent in the rod/cone/melanopsin-null mouse even though cryptochrome expression persists (89, 144), and mice lacking all cryptochromes exhibit a relatively normal PLR (207) and negative masking (131).

C. Behavioral Defects in the Physical Absence of ipRGCs

In addition to signaling intrinsic light detection to the brain, ipRGCs also relay signals originating in the rods and cones (11, 35, 43, 94, 149, 150, 228). Cell-ablation experiments have been carried out involving expressing diphtheria toxin (or its receptor, followed by acute toxin administration) under the melanopsin promoter, or by intraocular delivery of a melanopsin antibody coupled to the toxin saporin (64, 70, 85). These manipulations killed

60–95% of the ipRGCs, although the overall retinal morphology appeared normal (64, 70, 85). Specific ablation of the ipRGCs caused substantial defects in nonimage vision (64, 70, 85). When ablation was nearly complete, mice showed no circadian photoentrainment, no period lengthening in light-light (LL) conditions, and no negative masking; moreover, their PLR could attain only slight constriction in even the brightest light (Fig. 6*E*) (85). Thus killing the ipRGCs, hence eliminating their intrinsic photosensitivity and their conveyance of rod/cone signals to nonimage areas of the brain, produced some behavioral defects not unlike those shown by the triple-null mice lacking phototransduction in rods, cones, and ipRGCs. In other words, the ipRGCs constitute the key conduit for essentially all light signals to the brain for at least certain nonimage visual behaviors.

It is noteworthy that deficits in image vision were not detected following ablation of the ipRGCs, in that visual acuity, light/dark preference, optokinetic nystagmus, visual-cliff-test performance, water-maze navigation, and the electroretinogram all appeared normal (64, 70, 85). Conversely, rodless/coneless mice with ipRGCs being the only photoreceptors showed no detectable optokinetic nystagmus (25, 175). Thus ipRGCs are evidently not critical to image vision. Even so, they may still play a subtle role (see section VII, *A* and *B*, as well as Ref. 22).

From the above data, the role of conventional RGCs in the PLR and other nonimage functions has likewise been argued to be minimal (64, 70, 85). This is somewhat surprising, because conventional RGCs do innervate most of the brain centers for nonimage vision, some quite densely (9, 63, 75, 87, 130, 185). Conventional RGCs presumably do play a role in nonimage vision, although the degree of their involvement remains to be quantified.

The method of ablating ipRGCs by administration of saporin-conjugated melanopsin antibody has been extended to rats, where it produces a 70% depletion of melanopsin cells (95). Generalization of this approach to other species, especially primates, where ipRGC innervation of the dLGN may be significant, can lead to a greater understanding of these cells.

V. ELECTROPHYSIOLOGY OF INTRINSICALLY PHOTOSENSITIVE RETINAL GANGLION CELLS

A. Intrinsic Light Response

Light depolarizes the ipRGCs, same as for most invertebrate photoreceptors but opposite to the hyperpolarizing response of rods and cones (17, 35, 229). This depolarization is produced by an increase in a nonselective cation conductance (219).

1. Response to flashes of light—We begin by discussing the responses of ipRGCs to flashes of light. Flashes are defined as “impulse” stimuli when light intensity and duration can be proportionally interchanged without affecting the response amplitude or kinetics (10, 82, 117). Flashes are standard for studying rods and cones because the resulting “impulse responses” allow more straightforward quantitative analysis and, in principle, can predict the responses to more complex light stimuli if superposition is linear (39, 117).

Under voltage-clamp at room temperature, the ipRGC responds to a flash with a transient inward current that increases in amplitude with increasing flash intensity, ranging from a ~0.5-pA single-photon response (see below) to a saturated photocurrent of ~500 pA (Fig. 7, *A* and *B*) (39, see also Ref. 173). Also, the response time-to-peak shortens from ~3 s for the single-photon response to ~200 ms for a saturated response, reflecting light adaptation due to the speeding of the deactivation of the response (see below) (39, 227). The response is approximately threefold larger in amplitude and about threefold faster in kinetics near 37°C compared with room temperature (~23°C) (39).

The intensity-response relation for the ipRGC flash response at its transient peak can be described by the Michaelis equation, much as for rods and cones (Fig. 7*C*) (39, 117). The so-called "instantaneous" intensity-response relation (which is more revealing of the underlying activation mechanism), measured at a fixed time in the rising phase of the response, can be described by a saturating exponential function, again similar to the situation for rods (Fig. 7*C*) (39, 117). One interpretation of the saturating-exponential function is that each photoactivated melanopsin molecule activates a spatially restricted domain on the surface membrane within which phototransduction essentially saturates (117).

In the linear region of the flash intensity-response relation, a change in the flash intensity produces a proportional change in the flash response without a change in the response waveform (Fig. 7*B*) (39). A parsimonious interpretation of this linearity is that, at low intensities, the absorbed photons occur sufficiently far apart from each other that the associated phototransduction domains are spatially segregated and thus independent of each other. As such, although nonlinearities may exist in the phototransduction mechanism within individual spatial domains, the overall response is still just an arithmetic sum of the individual stereotypic responses, as long as domain overlap does not occur (117).

Half-saturation of the ipRGC flash response requires ~10^7 photons/μm^2 at the optimal wavelength (λ_{max}), or ~10^6-fold higher than for rods and ~10^4-fold higher than for cones at their corresponding λ_{max} values (Fig. 7*D*) (39). Thus ipRGCs are less sensitive than rods and cones (also see Refs. 35, 228), explaining why melanopsin-knockout mice show behavioral deficits primarily in bright light (89, 116, 133, 145). Because the flash response of ipRGCs is long-lasting (see below), however, the sensitivity to steady light is considerably boosted (see below).

2. Single-photon response

The single-photon response of mouse ipRGCs, that response triggered by a single photoactivated melanopsin molecule, reveals the phototransduction amplification with its amplitude and the phototransduction time course with its kinetics. This response is large, >1 pA at roughly body temperature, or larger than that of rods and 100 times that of cones (Fig. 7*E*) (39). Its waveform follows the convolution of two single-exponential decays (i.e., described by two time constants) (Fig. 7*B*), unlike the rod response, which requires four, and the cone response, which requires five, time constants. Two time constants suggest that there are two particularly slow steps in ipRGC phototransduction. In comparison, invertebrate single-photon responses (called quantum bumps) also have a more complex waveform (80). Moreover, the latter often have a highly variable latency following a flash and are of

variable and much larger amplitude (~50 pA in *Drosophila* and ~2 nA in *Limulus*), both not seen in the ipRGC (39, 80).

The ipRGC single-photon response is very slow. A useful metric for comparing the time courses of responses with different waveforms is the "integration time," given by the area under the response divided by the response peak (117). The mouse ipRGC single-photon response has an integration time of ~8 s at 37°C (39). This is 20 times that of rods and over 100 times that of cones. It is also much slower than the typical light response of invertebrate photoreceptors (80). A long integration time allows summation of photons arriving many seconds apart while making the cell insensitive to rapid fluctuations in light intensity. Thus ipRGCs are well-suited to reporting ambient light in the environment over a long time window.

3. Responses to steps of light

A flash of light is an instantaneous pulse of photons, while a step of light is a continuous shower. In a dim step of light, photon arrivals are infrequent, and the response of the cell is simply a random succession of single-photon responses. In a brighter light step, photon arrivals are frequent, and the single-photon responses overlap temporally and summate to produce a larger response. When the light step is intense enough to drive the cell response beyond its linear range, the response will be dictated by nonlinearities in the phototransduction cascade.

Adaptation also shapes the step response into a more complex form (39, 227) (Fig. 8). When stimulated by a long, bright step of light, the ipRGC voltage response rises to a transient peak and then relaxes to a lower level (35, 219, 227) (Fig. 8*B*). This relaxation is also observed for the intrinsic photocurrent recorded in voltage clamp and is thus due, in part, to adaptation in melanopsin phototransduction (219, 227) (Fig. 8*C*). Adaptation is also indicated by a shortening in the time to peak of responses to brighter flashes (Fig. 7*A*) (39), by an attenuation of the response amplitude to repeated flashes (227), and by a speeding of the incremental flash response in the presence of steady background light (227). In a way, it is surprising that ipRGCs light-adapt, because they are thought to signal the steady light intensity (17, 35), whereas adaptation, by definition, reduces the response in the presence of steady stimuli to favor the detection of changes, i.e., contrast (164, 218). The extent and role of adaptation in ipRGCs remain to be determined.

The response to a step of light will also be governed by the properties of melanopsin itself, especially for very bright stimuli. If melanopsin is bleached by light, then the effectiveness of photon capture should fall over time and reduce the photocurrent size, with the steady-state size determined by the equilibrium between bleaching and regeneration, in whatever way the latter happens. On the other hand, if melanopsin is bistable (see below), the step response should depend on the equilibrium between inactive and active melanopsin.

B. Melanopsin Density on ipRGCs

The effective density of melanopsin on the plasma membrane of ipRGCs (presumably only the M1 subclass studied so far) is very low, being of the order of several molecules per

square micron (39), or 10^4 times lower than the ~25,000 μm^{-2} for rod and cone pigments. In conjunction with their lack of membrane specializations for photon capture (11), such as the infoldings of plasma membrane found in cones or the stacks of intracellular discs found in rods, this low pigment density underlies the low sensitivity of ipRGCs, despite a large single-photon response. Indeed, it is the large, detectable single-photon response of ipRGCs (resolved directly or by fluctuation analysis) that has allowed an estimate of the melanopsin density (39), which is otherwise difficult to measure with microspectrophotometry or biochemistry owing to the paucity of cells and the low melanopsin density. With the average surface area of an M1 cell being ~10^4 μm^2, this density corresponds to a total of 10^4–10^5 melanopsin molecules/cell (39). The density is likely to be even lower for the other ipRGC subclasses (see above).

IpRGCs have thus adopted a different strategy from cones for reducing sensitivity. Cones capture light nearly as well as rods but are 100-fold lower in sensitivity because they produce a tiny single-photon response. The fact that ipRGCs combine a low effectiveness of photon capture with a large single-photon response is intuitively appealing; namely, because light has to pass through ipRGCs before reaching the rods and cones, a low melanopsin density minimizes interference with image vision. Rods and cones, in turn, drive ipRGCs in low light conditions to endow these nonimage photoreceptors with a large overall dynamic range.

C. Voltage Response and Spike Generation

Rods not only have large single-photon responses, but also faithfully transmit them to postsynaptic cells, partly because they signal in an analog (graded) fashion, which does not possess a threshold (50, 90, 171). IpRGCs signal digitally via spikes, with a firing threshold that could, in principle, limit sensitivity. Nonetheless, at least the M1 cells appear to be also capable of signaling single-photon absorption by increasing their spike rate (39). This ability is likely brought about by the high input resistance of the cell, with ~1 GΩ being not uncommon even for an intact cell in the flat-mount retina (39, 173). Also, its slowness makes the single-photon response unlikely to be filtered by the membrane time constant regardless of its location of origin on the cell (39). Equally importantly, ipRGCs show spontaneous firing in darkness and in the absence of synaptic activity (39), reflecting their membrane potential intrinsically hovering near firing threshold and occasionally crossing it. Thus a single-photon response needs only to bias the cell to cross threshold more often (39). In a number of other neuronal types, a current of just several picoamperes is also sufficient for driving spike activity (38, 97, 188).

The ability of ipRGCs to increase their spike rate in response to single-photon absorption helps signaling tremendously. It is estimated that, on average, a few hundred ipRGCs are activated by a “threshold” diffuse light that elicits a just-detectable PLR in rodless/coneless mice (39). If each ipRGC were to require five single-photon responses instead of one to signal, the Poisson distribution predicts that there would not be even one ipRGC active at this threshold light intensity (39). Finally, if the ipRGC were more like a textbook neuron, namely, with a resting potential of −70 mV, a spike threshold around −40 mV, and an input resistance of 1 GΩ, then 30 single-photon responses would be required for driving spiking.

Accordingly, the ipRGC-driven light threshold of the PLR would have to be many orders of magnitudes higher.

Spontaneous firing of ipRGCs in darkness has been observed in different preparations and with different recording methods: multielectrode-array, whole cell, perforated-patch, and loose/cell-attached patch recordings (17, 39, 174, 205). In addition to its observation in the whole retina, spontaneous firing has been reported in dissociated cells, suggesting that it is not simply due to inadequately blocked synaptic excitation, although the cause of spontaneous activity in situ and after dissociation may not be the same (39).

The mechanisms of spontaneous as well as synaptically driven activity in the ipRGCs are certain to involve voltage-gated and other ion channels, which remain to be studied. These may differ between subclasses of ipRGCs. For instance, it was mentioned earlier that M1 cells are more prone to depolarization block than M2 cells, which can sustain higher rates of firing (173).

D. Correlating ipRGC Activity With Behavior

The influence of ipRGC intrinsic photosensitivity on behavior can be teased from that of rods and cones based on absolute sensitivity, spectral response, and kinetics. Gamlin and colleagues (56, 126) have used this approach to demonstrate that melanopsin signaling does make a substantial contribution to the primate PLR under normal conditions (56, 126). Some aspects of the reflex can be attributed to melanopsin signaling alone, even though the rods and cones are present and functional (but nonetheless light-adapted). For instance, in the macaque, the pupil takes some time to dilate after the stimulus has been switched off. This poststimulus, sustained response is insensitive to pharmacological block of rod and cone signals and has an action spectrum matching that of the ipRGC intrinsic photosensitivity (56). The same is true for the PLR of humans (56, 126, 231). Other details of melanopsin signaling have also been reported to manifest in the PLR (134). It remains to be seen whether these responses can be used as a diagnostic of ipRGC health and function (101).

As described earlier, rodless/coneless mice allow the impact of ipRGCs on the whole animal to be examined in isolation. For instance, by comparing the number of ipRGCs active at the PLR threshold of rodless/coneless mice to the number of rods active at the reflex threshold of wild-type mice (which is rod-driven), it has been estimated that the intrinsic photosensitivity of one ipRGC can drive this behavior as powerfully as a very large number of rods (39). How powerfully ipRGCs signal in the wild-type animal, when their intrinsic photosensitivity acts in concert with synaptic excitation from rod and cone pathways and when conventional RGCs are also active, will require additional investigation.

Study of ipRGC-driven functions in rodless/coneless mice may pertain to “blind” patients who rely exclusively on melanopsin signals for photodetection (34, 103, 232). These people have lost image vision owing to rod/cone degeneration, but some are still able to photoentrain their circadian rhythm (and therefore get over jetlag, for example), constrict their pupils, and even have some reported visual awareness, with the spectral sensitivity of these remaining functions corresponding to that of the ipRGC intrinsic photosensitivity (103, 232).

VI. PHOTOTRANSDUCTION BY INTRINSICALLY PHOTOSENSITIVE RETINAL GANGLION CELLS

How photoisomerized (i.e., activated) melanopsin increases membrane conductance in the ipRGCs is an active area of research (Fig. 9). Melanopsin is akin to invertebrate photopigments (12, 155), and most invertebrate photoreceptors also depolarize to light. Thus it is not surprising that efforts on this question have been guided partly by analogy to invertebrate phototransduction (65, 83, 127, 143, 161, 177, 220). Invertebrate phototransduction is best understood in *Limulus* and *Drosophila* photoreceptors, which share the features of a bistable visual pigment coupled via G_q to a phospholipase C signaling cascade, leading to the opening of nonselective cation channels (47, 229). How PLC is coupled to the transduction channels remains unclear (80). PLC cleaves phosphatidylinositol 4,5-bisphosphate (PIP_2) to generate inositol trisphosphate (IP_3) and diacylglycerol (DAG). IP_3 typically causes intracellular Ca^{2+} release, while DAG can activate PKC or be further metabolized to yield physiologically active arachidonic acid (AA) and other polyunsaturated fatty acids (PUFAs). IP_3 appears to be the second messenger for phototransduction in *Limulus* photoreceptors (47, 229). In *Drosophila*, however, phototransduction appears to be via a membrane-delimited pathway involving PIP_2, DAG, and/or PUFAs (47, 80, 146, 229). The transduction channels themselves are also heterogeneous. *Drosophila* utilizes TRP and TRPL channels (80). In *Limulus*, three transduction channel types have been discriminated but not molecularly identified, although TRP channels appear to be expressed in the ventral eye (47, 229).

In contrast, vertebrate rod and cone phototransduction involves a bleachable photopigment, G_T (transducin), and a phosphodiesterase (PDE) that hydrolyzes cGMP. cGMP keeps the nonselective cation CNG channels open in darkness, and light triggers cGMP hydrolysis by activating the PDE to lead to channel closure and a membrane hyperpolarization (47, 117, 229).

The components of ipRGC phototransduction are described one by one below, granted that many details are still far from clear.

A. Molecular Components of Phototransduction

1. Melanopsin—Melanopsin belongs to the rhabdomeric group of visual pigments, which are found predominantly in invertebrates (47, 229), with a signature being an unusual tyrosine residue in the counterion position for the Schiffbase linkage between the chromophore and the opsin protein (155, 156). Melanopsin's extraordinarily long intracellular tail has a number of potential phosphorylation sites (155), and it is glycosylated (45).

There are two sets of melanopsin genes, *opn4m* and *opn4x* (12). Mammals appear to have only one melanopsin gene, of the *opn4m* type, while some other vertebrates have both *opn4m* and *opn4x*, or even more than one of each (12, 13). Compounding this genomic diversity, melanopsin transcripts can be diverse. The mouse has two melanopsin isoforms from alternative splicing: a short and a long form differentially expressed in subclasses of

ipRGCs (152). Whether there is a corresponding functional diversity is unknown. In mammals (both placental and marsupial), melanopsin expression appears restricted to RGCs (35; but see Refs. 37, 55, 78, 88, 147, 153, 156, 180). In lower vertebrates, however, both *opn4m* and *opn4x* are expressed fairly widely in the retina as well as in other tissues such as the pineal gland, iris, brain, and skin (4, 12, 29, 30, 41, 53, 67, 93, 98, 155, 198–200). Melanopsins have also been identified in invertebrates (105, 209).

In the early days, there was some uncertainty about whether melanopsin was the signaling photopigment or merely an accessory entity required for photosensitivity in ipRGCs. Part of this uncertainty arose from an early report that melanopsin was expressed also in the retinal pigment epithelium (RPE) (147), a site for the regeneration of the chromophore and therefore of rod and cone pigments (but see Ref. 55). This report led to the speculation that melanopsin might act as a photoisomerase that regenerates the chromophore simply by absorbing a photon (147). At one point, the absorption spectrum of biochemically purified melanopsin (with λ_{max} at ~420 nm) also did not match the action spectrum of ipRGCs (λ_{max} ~ 480 nm) (139).

That melanopsin is indeed the signaling photopigment was subsequently supported by experiments showing that its expression conferred photosensitivity to otherwise photo-insensitive HEK 293 cells, *Xenopus* oocytes, and Neuro-2A cells (Fig. 9*A*) (127, 143, 161). The action spectrum obtained from these heterologous expression systems (127, 143, 161) also largely (though not uniformly) matched that of the native ipRGCs (17, 35, 205) (Fig. 9, *B* and *C*). Moreover, exogenously administered chromophore was unable to restore photosensitivity in melanopsin-knockout ($opn4^{-/-}$) mice, suggesting that melanopsin was not simply acting as a photoisomerase (55). Finally, the absorption spectrum of biochemically purified melanopsin from native ipRGCs has since been found to peak near 480 nm at least under some experimental conditions (105, 213). The photochemical characteristics of melanopsin are still being worked out. The possible bistability of this protein will be discussed later.

2. G protein—Visual pigments are prototypical G protein-coupled receptors. Melanopsin has been reported to activate G_T and G_q in vitro (139, 193). In heterologous expression systems, melanopsin signaling is likewise blocked by antagonists of G protein signaling (127, 143, 161). IpRGC phototransduction is also blocked by intracellular GDPβS dialysis, known to block G protein signaling (65, 220) (Fig. 9*D*). However, paradoxically, intracellular GTPγS dialysis also blocks phototransduction (but not via occlusion) instead of activating it as might be expected from GTPγS being a G protein activator (220). Specific G protein antagonists support the involvement of G_q family members, with GPant-2, pertussis toxin, and cholera toxin (which target G_i, G_o, and G_s) having no effect in cultured ipRGCs (65), but GPant-2a (which targets $G_{q/11}$) virtually abolishing the photocurrent (65) (Fig. 9*D*). IpRGCs also express mRNA for the G_q family members: most prominently G_{14}, followed by G_q, G_{11}, and G_{15} (65). Expressions of these isoforms have yet to be confirmed at the protein level, and their actual participation in phototransduction should be examined with loss-of-function approaches. IpRGCs certainly do not appear to use rod transducin, as they function normally in mice that lack this protein ($Gnat^{-/-}$) (89).

3. Effector—Attention has focused on phospholipase C (PLC) because of its involvement in invertebrate phototransduction, especially PLCβ, which is activated by G$\alpha_{q/11}$. In cultured ipRGCs, melanopsin phototransduction is blocked by U73122, which targets PLC, but not by U73343, an inactive homolog (65) (Fig. 9E). All ipRGCs examined show expression of PLCβ, with PLCβ4 being the most abundant, followed by PLCβ1, PLCβ3, and PLCβ2 (65). Incidentally, the photosensitivity of chicken melanopsin RGCs is also susceptible to blockers of the PLC cascade (32).

Protein Kinase Cζ (PKCζ) is enriched in ipRGCs, and a PKCζ-knockout mouse has deficits in nonimage vision (148). Because PKCζ lacks binding domains for DAG and Ca^{2+}, it is unlikely that this enzyme is activated by the early products of PLC catalysis. Incidentally, PKC also appears to be important for melanopsin phototransduction in *Xenopus* melanophores (96) and may play a role in phototransduction in invertebrate photoreceptors (47, 229).

4. Second messenger—Despite PLC's apparent involvement in melanopsin phototransduction, the downstream messenger of excitation is still unknown. Melanopsin phototransduction has been reported to persist in excised patches, presumably ruling out any cytosolic messenger (65). On the other hand, the photocurrent does gradually decrease or disappear altogether in whole cell recording (but not perforated-patch recording) of ipRGCs, possibly reflecting the washout of cytosolic components by the pipette solution (17, 39, 220).

One product of PLCβ activity is IP_3, which mobilizes intracellular Ca^{2+}. On the other hand, intracellular dialysis with IP_3 neither activated a current nor occluded phototransduction, and depletion of intracellular Ca^{2+} stores did not block phototransduction (65, 83, 177). It was also reported, however, that strong chelation of intracellular Ca^{2+} by BAPTA reduced or eliminated the photocurrent in ipRGCs, although this effect may not directly involve phototransduction (65, 220). At least in *Xenopus* melanophores and *Amphioxus* melanopsin photoreceptors, Ca^{2+} does appear important for melanopsin phototransduction (60, 96). Apart from producing IP_3, PLCβ depletes PIP_2 in the plasma membrane and generates DAG. Wortmannin, which inhibits PIP_2 synthesis, has complex effects on ipRGCs (65). There was no detectable effect of exposing ipRGCs to DAG and analogs of DAG (65; but see Ref. 220). In sum, the exact second messenger is unclear.

5. Conductance—By analogy to *Drosophila* phototransduction, it has been widely speculated that the nonselective cation conductance mediating ipRGC phototransduction is a TRP channel. Attention has focused on TRPC channels, which are the most homologous to the *Drosophila* phototransduction channels (TRP and TRPL) and are activated by PLC signaling (162). Indeed, putative TRP-channel antagonists applied to ipRGCs blocked the photoresponse (83, 177, 220). Unfortunately, agonists and antagonists of TRP channels are notoriously nonselective (162).

Localization data are also controversial. One report described TRPC6 immunoreactivity in ipRGCs (and in a large number of conventional RGCs; Ref. 220), whereas another described immunoreactivity for TRPC7 but not TRPC1, TRPC3, TRPC4, or TRPC6 (177). TRPC7

transcript does appear to be enriched in ipRGCs compared with conventional RGCs, unlike TRPC3 and TRPC6 (83). These findings have yet to be confirmed with loss-of-function studies.

What does seem clear is that the CNG channels mediating phototransduction in rods and cones are not present in ipRGCs. Exposing ipRGCs to CNG-channel antagonists had little effect on phototransduction (177, 220), and ipRGCs are not immunoreactive for CNGA1, CNGA2, or CNGA3. Finally, the *CNGA3*$^{-/-}$ mouse has normally functioning ipRGCs (89, 220).

Not much is known about the transduction conductance biophysically, such as with respect to ionic selectivity, unitary conductance, and possible voltage dependence. There are intriguing beginnings (Fig. 9*F*). For instance, the photocurrent has been reported to be unchanged when all sodium is removed from the bath (219).

6. Remarks—Our understanding of phototransduction in the ipRGCs has been hampered by the rarity of these neurons, which limits biochemical and some molecular approaches to the problem. This difficulty is compounded by heterogeneity in the ipRGC population, which potentially has correlates in the phototransduction mechanism as well. Incidentally, a most dramatic recent finding may bear on this problem. It was found that, after viral transduction to express melanopsin, conventional RGCs became intrinsically photosensitive, in a manner strikingly reminiscent of the native ipRGCs (Fig. 14) (111). Thus, potentially, many melanopsin phototransduction components preexist in conventional RGCs. If so, the specific expression of particular proteins in ipRGCs would no longer be a good criterion or guide for probing the molecular mechanism of phototransduction.

B. Chromophore-Opsin Interaction

A photopigment consists of the opsin apoprotein covalently linked to the chromophore, which is 11-*cis*-retinal (at least for land-based and marine vertebrates; many freshwater vertebrates use a structural variant). Light isomerizes the chromophore from 11-*cis*-retinal to all-*trans*-retinal, consequently driving conformational changes in the opsin to eventually an active state. The fate of the pigment afterwards has broad consequences. Rod and cone pigments are bleachable, in that the photoisomerized chromophore ultimately dissociates from the opsin, rendering the latter nonphotosensitive. A complex cycle of enzymatic reactions is required for regenerating 11-*cis*-retinal. Meanwhile, the bare opsin (i.e., after chromophore dissociation) has constitutive activity, which desensitizes the cell and accelerates its response kinetics. The binding of chromophore, which acts as an inverse agonist, simultaneously quenches this constitutive activity and makes the opsin functional as a photopigment again. An advantage to having the photoreceptors on the “wrong” side of the retina, i.e., not facing the incident light, is that their photosensitive outer segments can be intimately associated with the RPE, which is a primary site of chromophore regeneration. The photopigments of *Limulus*, *Drosophila*, and other invertebrates are quite different. They are bistable, meaning that the isomerized chromophore does not dissociate from the opsin. Instead, the thermally stable inactive and active (“meta”) states of the pigment simply interconvert, primarily through light absorption (reviewed in Refs. 47, 91, 229).

Accordingly, invertebrate photoreceptors such as those in squid can face the incident light, as the ipRGCs do.

One direct way of demonstrating pigment bistability is with spectrophotometry, with light driving the pigment back and forth between the thermostable inactive and active states each with a characteristic absorption spectrum. In such a manner, *Amphioxus* melanopsin was demonstrated to have an inactive state with a λ_{max} at 485 nm and an active (meta-) state with a red-shifted λ_{max} (105). Nonetheless, *Amphioxus* is an invertebrate (60, 105), and mammalian melanopsin may be different (12, 105) (see above). Spectrophotometric work on the question of bistability of mammalian melanopsin has not been carried out. Light does drive the formation of a spectrally distinct, red-shifted state of mouse melanopsin, but it is unclear whether it is thermally stable (212). All melanopsin isolated from dark-adapted retina is bound to 11-*cis*-retinal, suggesting that there is at least a light-independent pathway for melanopsin regeneration (212). One difficulty in studying melanopsin in situ with microspectrophotometry is that the pigment is present in insufficient quantity (see above).

Some evidence for bistability of vertebrate melanopsin has come from in vivo experiments on the photic modulation of spiking of SCN neurons, the PLR, and negative masking (135). The principal finding is that a long-wavelength conditioning light potentiates these phenomena. Because the λ_{max} of meta-melanopsin is believed to be red-shifted from that of melanopsin, this potentiation has been taken to mean that the conditioning light drives more meta-melanopsin back to the resting state, where it is ready for light absorption and activation, thereby increasing sensitivity. These data appear compelling, especially because this potentiation is absent in mice lacking melanopsin (135). The PLR has even been used to determine the action spectra for melanopsin and meta-melanopsin (134). On the other hand, no such potentiation has been observed in the spiking activity of the ipRGCs themselves (124), and potentiation of the intrinsic photocurrent by long-wavelength conditioning light is not obvious (39).

While failure to observe direct long-wavelength potentiation of the ipRGCs argues against a role for melanopsin bistability under the stimulus paradigms used, several factors conspire to make bistability difficult to observe. First, sufficient inactive (but ready to be activated) melanopsin must be generated by the conditioning stimulus to produce an observable effect (i.e., a larger photocurrent for a given test stimulus). This requires that the absorption spectrum of meta-melanopsin be distinct enough from that of melanopsin for selective stimulation. It also requires that sufficient meta-melanopsin exists at the beginning of the experiment for conversion back to the inactive state. Finally, the conditioning stimulus must be bright enough to isomerize a large percentage of this meta-melanopsin. There has been a preliminary report of melanopsin bistability observed in mammalian ipRGCs, although these data are not yet published (160).

All-*trans*-retinal has also been shown to increase the photosensitivity of heterologous systems expressing melanopsin and that of the ipRGCs (55, 58, 127, 143). The interpretation is that bare melanopsin can bind all-*trans*-retinal; the chromophore is then photoisomerized to 11-*cis*-retinal, and the holopigment becomes capable of driving phototransduction upon subsequent photon absorption. However, there is a finite probability that all-*trans*-retinal

itself is photoisomerized directly (i.e., without being bound to melanopsin) to a number of *cis*-forms, some of which are known to bind melanopsin (212).

In a heterologous-expression system, melanopsin does appear to be capable of existing in the bare form in that it can bind to exogenously applied chromophore [11-*cis*-retinal, the native chromophore (212), or 9-*cis*-retinal, a readily available analog] to form a functional photopigment (127, 143). Exogenous chromophore also increases the sensitivity of ipRGCs severalfold (39, 55). These results do not prove that melanopsin releases chromophore on photostimulation, as the increase in sensitivity could be due to the exogenous chromophore binding to opsin that was bare to begin with, regardless of the light history of the cell. In spite of ipRGCs being physically far removed from the RPE, any bleaching of melanopsin may not be a big issue. It has been shown that ipRGCs still retain some of their intrinsic photosensitivity even after the classical visual cycle in the RPE has been disabled genetically or pharmacologically, suggesting that they have access to an alternative chromophore source or regeneration mechanism (40, 204). Indeed, Müller glial cells are able to regenerate chromophore for cones (216, 217) and, although these cells are not tightly associated with conventional RGCs, they do appear to be intimately associated with ipRGCs (208). There might also be an intrinsic chromophore-regeneration mechanism within the ipRGCs themselves.

In summary, it remains an open question whether melanopsin is bleachable or bistable. A classical test of pigment bistability in intact photoreceptors, as has been done in invertebrates, is to generate a "prolonged depolarizing afterpotential" with a pulse of intense light near the optimal excitation wavelength, followed by a second intense light pulse at a different, typically longer wavelength, to see if the prolonged response can be cut short (91, 160). This idea is a variation of the concept of photointerconversion between the inactive and active pigment states described above; namely, the first pulse drives so much photopigment into the meta-state that the downstream deactivation steps are overwhelmed, allowing prolonged activation of phototransduction by the thermally stable meta-state; the second pulse drives the meta-state pigment back to the inactive state, thus truncating phototransduction (91). Finally, it might be pointed out that bistability and bleaching need not be completely mutually exclusive.

VII. INTRINSICALLY PHOTOSENSITIVE RETINAL GANGLION CELLS AND RETINAL CIRCUITRY

A. Synaptic Drive to ipRGCs

The spectral sensitivities of circadian photoentrainment and other nonimage visual behaviors in wild-type animals have components of rod, cone, and ipRGC action spectra (154, 195, 197, 202). As mentioned above, in mice lacking ipRGC photosensitivity, the functions of circadian photoentrainment, negative masking, and the PLR remain, albeit incomplete. The same is true for mice lacking rod/cone signaling but retaining ipRGC function. Apart from their intrinsic photosensitivity, ipRGCs are also influenced by rod and cone circuitry in the retina (64, 70, 85). Therefore, it is important to understand how rod and cone signals drive the ipRGCs.

Multiple techniques have been used to examine this question, including a relatively uncommon approach that employs a Bartha strain of pseudorabies virus (PRV152), which spreads through neuronal circuits transynaptically in a retrograde fashion (26, 151, 184). When injected into the anterior chamber of one eye, the virus infects the ciliary ganglion and traverses the Edinger-Westphal complex to reach retinorecipient structures including the OPN, SCN, and IGL. There, the virus is taken up by the synaptic terminals of RGCs projecting to these structures from both the injected eye and the uninjected contralateral eye. Within ~4 days of injection, virtually all labeled RGCs in the contralateral eye are ipRGCs (208). The virus continues to spread to neurons presynaptic to these ipRGCs (151). In this way, local circuits of ipRGCs can be explored. Some viral transduction may also occur in the absence of synapses, as Müller glial cells have been labeled, and these are unlikely to synapse onto RGCs (138, 208). We shall begin this section with the anatomy discovered by the use of PRV and other techniques, followed by the physiology of excitatory, inhibitory, and modulatory synapses onto ipRGCs.

1. Anatomy—The dendrites of RGCs and the axon terminals of bipolar cells are situated in the IPL (see above). The IPL has two major subdivisions: the ON-sublamina closer to the GCL and containing axon terminals from ON-bipolar cells (which depolarize in response to light increment), and the OFF-sublamina closer to the INL and containing terminals from OFF-bipolar cells (which depolarize in response to light decrement) (Fig. 10). ON-RGCs depolarize to light because their dendrites stratify in the ON-sublamina and receive excitatory input from ON-bipolar cells. Similarly, OFF-RGCs stratify in the OFF-sublamina and receive excitatory input from OFF-bipolar cells. Such an arrangement is a rule in the retina (121), but ipRGCs are an exception (43, 94).

The M1 (i.e., OFF-stratifying) subtypes of ipRGCs send their dendrites past the ON-sublamina and arborize in the OFF-sublamina (Fig. 10). Although these cells do receive some input from OFF-bipolar cells in the OFF-sublamina as expected, this OFF-input is substantially weaker than the input from ON-bipolar cells (228). Even more strangely, the M1 ipRGC receptive field defined by ON-bipolar cell inputs corresponds to its entire dendritic field in both the ON- and OFF-sublaminae rather than to just the proximal dendrites traversing the ON-sublamina (228). As it turns out, some ON-cone bipolar cells (but not rod bipolar cells, see Ref. 43) actually form ribbon synapses, albeit unconventionally, with ipRGC dendrites in the OFF-sublamina (Figs. 10 and 11) (43, 94). These ectopic synapses are made en passant from the ON-bipolar cell axon itself or small lateral extensions from the axon at the level of the OFF-sublamina (Figs. 10 and 11) (43, 94). How these bipolar cells relate to the known subtypes in rodent (44, 57) is not obvious, but they may correspond to type 6 and/or 8 bipolar cells, and possibly also type 7 (11, 43, 208). Because cone-driven ON-bipolar cells in mammals also convey signals from rod bipolar cells (121), the above circuitry to the M1 ipRGCs does include rod signals. Likewise, OFF-cone bipolar cells would be expected to convey rod signals to ipRGCs. In rat, however, rod bipolar cells are reported to also contact ipRGCs (M1 cells and possibly others) directly by ribbon synapses at their somata and proximal dendrites in the ON-sublamina (Fig. 10) (142, 228). This connection is nonetheless unusual because rod bipolar cells are generally believed not to contact RGCs directly, but only indirectly through a

circuit involving cone bipolar cells and AII amacrine cells (121). The above conclusions are mostly based on co-localization studies with pre- and postsynaptic markers under light microscopy. However, electron microscopy has also been used in some cases (11).

For primate ipRGCs, as in rodent, the ON-cone pathway drives the ipRGC over its entire dendritic arbor (35). Presumably, the ON-bipolar cells also make en passant synapses to the ipRGCs in the OFF-sublamina. Indeed, bipolar synapses were observed over the entire dendritic arbor of the ipRGCs (99). In primate, M1 ipRGCs receive an approximately twofold lower density of synapses than the M2 (i.e., ON-stratifying) ipRGCs (99). Synaptic drive may thus be more important to the M2 cells, possibly to compensate for the lower intrinsic photosensitivity of these cells observed at least in mouse (173). The primate ON-bipolar cells presynaptic to the ipRGCs may be the DB1, DB6, and/or giant bistratified bipolar cells, both of which may costratify with the ipRGC dendrites (20, 36, 92, 99, 120). Finally, primate ipRGCs also receive OFF-input from the S-cone pathway that is likewise coextensive with the dendritic field (35).

In both rodent and primate, all ipRGCs are contacted by amacrine cells, at a density exceeding that of bipolar cell synapses (11, 99). The different subtypes of ipRGC also appear to interact with different amacrine cell subtypes (208). For example, the rodent M2 ipRGCs are postsynaptic to a monostratified amacrine cell (Fig. 10) (208). This is not true of the M1 ipRGCs, which are postsynaptic to dopaminergic amacrine (DA) cells (142, 208, 211) (and, in turn, also drive the DA cells reciprocally; see below and Fig. 10). Interestingly, the DA cells are also driven by the ON-pathway despite having dendrites in the OFF-sublamina of the IPL (235). In fact, the same ON-bipolar cells drive both the ipRGCs and the DA cells with ectopic synapses (Fig. 10) (43, 94).

2. Physiology of excitatory inputs—Rodent ipRGCs receive synaptic excitation even in darkness (149, 228). Their spontaneous excitatory postsynaptic currents (EPSCs) are comparable to those of conventional RGCs (149). Light exerts a net synaptic excitation of the ipRGCs (228) (Fig. 12). The synaptic input is many orders of magnitude more light sensitive than the intrinsic photosensitivity of ipRGCs, conferring an overall light sensitivity comparable to conventional RGCs (223, 228). Interestingly, while the synaptic input to conventional RGCs is transient, that to ipRGCs is largely sustained (Fig. 12*D*) (228). Thus ipRGCs are suited to signaling over long durations, both in their intrinsic photosensitivity (17, 35, 39) and in their synaptic inputs (228).

Rodent ipRGCs also receive a minor input from OFF-bipolar cells, obvious only in an extensive pharmacological cocktail that blocks almost everything except glutamatergic transmission (228). Small and rarely observed in control conditions, the OFF-response is of uncertain importance, perhaps making some contribution to spiking at light offset (228).

Primate ipRGCs show a strong, rod-driven excitation that is ~5 log units more sensitive than the intrinsic photoresponse and is near the absolute threshold for human vision (Fig. 12*C*) (35). Overall, the synaptic input to ipRGCs is broadly similar to that of mouse, with the exception that both ON and OFF responses are prominent, the latter originating from blue

(S) cones (35) (Fig. 12, *A* and *B*). Moreover, the cone inputs are transient, but compensated by the sustained excitation from the intrinsic light response (35).

3. Physiology of inhibitory inputs—IpRGCs also receive a continuous barrage of spontaneous inhibitory postsynaptic currents (IPSCs) in darkness, influencing the dark membrane voltage and input resistance of these neurons (149, 228). IPSCs appear to dominate over EPSCs in darkness (228), and blocking them increases spontaneous firing activity of the ipRGCs (228). The IPSCs are much smaller in ipRGCs than conventional RGCs (149) and, being blocked completely by bicuculline, appear to be mediated solely by $GABA_A$ receptors (149). IpRGCs do express functional glycine receptors, but curiously, antagonists of glycinergic transmission produced no change in the spontaneous and light-evoked synaptic currents of these cells (149, 228). For the M1 ipRGCs, the IPSCs may originate in part from DA cells, which corelease GABA and are spontaneously active (33, 49, 104, 208, 221, 235). For the M2 ipRGCs, as mentioned above, they are contacted by a monostratified amacrine cell (208).

Light also drives IPSCs (149, 208, 228). The inhibition appears to make the light response more transient at low light intensities, improving the temporal resolution of ipRGCs (228). The inhibition also reduces depolarization block at high light intensities, extending the dynamic range of the ipRGCs (228).

The ipRGCs of primates showed no evidence of an inhibitory surround typical of most conventional RGCs (35). They do receive inhibitory synapses, although these have yet to be characterized electrophysiologically (99). The amacrine cells giving rise to these synapses are also unidentified, although the DA cells are candidates owing to costratification of their dendrites with those of ipRGCs (36).

4. Modulatory inputs—As mentioned above, DA cells are presynaptic to the M1 ipRGCs and release both dopamine and GABA (Fig. 10) (33, 104, 211, 221). Dopamine appears to upregulate the melanopsin transcript (169). For example, intraocular injection of kainate produces a massive degeneration of the INL, including the DA cells, and results in a reduction of the melanopsin transcript and protein (169). Subsequent intraperitoneal injection of a D2 agonist increases melanopsin mRNA, and ipRGCs do appear to express D2 receptors (169).

B. Synaptic Drive of Retinal Circuitry by ipRGCs

The canonical pathway of information flow through the retina leads from the outer retina, where the rods and cones initiate the light signals, to the inner retina, where the RGCs transmit the signals to the brain (121). With the discovery of ipRGCs, it became apparent that light signals could also originate in the inner retina. Further work on the ipRGCs has shown that these atypical signals not only proceed centripetally to the brain, but also centrifugally back to the outer retina where the rods and cones lie (234).

1. Modulation of cone signaling—The first suggestion of centrifugal signal-flow from ipRGCs within the retina arose from studies of the human electroretinogram (ERG), which measures concerted activity of the retina in response to light. At night, in the presence of

background light that saturates the rods, the isolated cone ERG shows a delayed b-wave peak (which reflects ON-bipolar cell activity), suggesting that the processing of cone signals is slowed. This delay can be attenuated by prior light exposure. The light effect has low photosensitivity, long temporal integration, and a spectral sensitivity with λ_{max} ~480 nm. This effect is much more prominent in the ipsilateral eye, suggesting a strong component that does not require circuitry in the brain. Therefore, light signaling by ipRGCs may modulate cone signal processing in the human outer retina (71).

The situation is slightly different in mice. The ERG does display a circadian variation in the cone b-wave (with the rods saturated) that is attenuated by light exposure. However, this attenuation persists in the *Opn4*$^{-/-}$ mouse, which lacks melanopsin (8). Nonetheless, the diurnal variation in the cone b-wave is reduced in this mouse line, suggesting that melanopsin signaling may still have a role (8). These studies suggest another connection between melanopsin signaling and image vision.

2. Electrical synapses with retinal neurons—There is evidence that ipRGCs are coupled to other, nonintrinsically photosensitive retinal neurons by electrical synapses. Ca^{2+} imaging of flat-mount mouse retinas lacking rods and cones (*rd/rd cl*) revealed a population of cells in the GCL that were sensitive to light (176). Upon addition of carbenoxolone, which blocks gap junctions, this population of photosensitive cells was halved (176). This effect was not observed with blockers of ionotropic or glutamatergic signaling, nor with cadmium, which would globally inhibit chemical synaptic transmission by blocking voltage-gated Ca^{2+} channels (176). The interpretation is that the ipRGCs, those cells that remain photosensitive in carbenoxolone, drive through gap junctions a population of GCL neurons, which may be ganglion cells and/or displaced amacrine cells. Indeed, whole cell recording in mice has shown that the superfusion of another gap junction blocker, meclofenamic acid, decreases membrane capacitance and increases input resistance, also consistent with electrical coupling of ipRGCs to other cell types (174).

Despite some coupling to other cells, ipRGCs in mouse, rat, and primate do not appear to be strongly connected to one another by gap junctions, as their intrinsically driven receptive fields are coextensive with their dendritic fields (35, 227), and no correlated firing has been detected in simultaneous recordings of adult ipRGCs in multielectrode recordings (205, 224). Studies using neurobiotin to fill mouse ipRGCs also have not explicitly reported dye-coupling with other ipRGCs (173, 174). Knowing the role of ipRGC electrical synapses awaits identification of the coupled cells and their physiology.

3. Drive of dopaminergic amacrine cells—Not only do M1 ipRGCs appear to be postsynaptic to DA cells (see above), there is strong evidence that they drive the DA cells as well, presumably via reciprocal synapses (Fig. 10) (but see Refs. 28, 210, 234). Dopamine has diverse effects in the retina, serving as a widespread signal for light adaptation, and DA cells are its only source (226). Three subtypes of DA cells have been described in the murine retina by electrophysiology: those insensitive to light, those responding to light with a transient elevation of spike frequency, and those responding to light with a sustained elevation of spike frequency (235). The sustained DA cells (sDA cells) are photosensitive even in the presence of L-AP4, which blocks the ON-pathway of rod and cone signaling

through the retina, but lose the photosensitivity under complete blockade of glutamatergic signaling (234). Thus they are driven by a rod- and cone-independent glutamatergic synapse. The presynaptic neurons appear to be ipRGCs, based on the following evidence. First, the light response of the sDA cells persists under blockade of rod/cone signals as well as in rodless/coneless mice (234) but are absent in melanopsin knockout mice (D. G. McMahon, personal communication). The spectral sensitivity of the light response is also roughly fit by the 480-nm nomogram characteristic of melanopsin and ipRGC photosensitivity (234). Finally, the sensitivity and kinetics of the light response are reminiscent of those of the ipRGCs, being low and sluggish, respectively (234). The reciprocal interaction between ipRGCs and sDA cells may be complex, because ipRGCs activate sDA cells, and sDA cells might both inhibit ipRGCs through GABA release and sensitize them by upregulating melanopsin expression through dopamine release (see above, and more below). Excitation of the sDA cells by ipRGCs is an example of unusual signaling from the inner to the outer retina.

C. Long-Term Interactions Within the Retina

Light regulates melanopsin expression. Under a variety of light-dark cycles, melanopsin mRNA rises at the onset of light and reaches a peak near the transition to darkness (76, 123, 170). As a consequence, melanopsin protein is higher during the day (76). Rods and cones have a role in this regulation (170, 214), possibly through stimulation of dopamine release (169). This diurnal variation in melanopsin, in addition to being dictated by light, is also under control of the circadian clock (but see Refs. 123, 170). A higher level of melanopsin expression would be expected to improve photon-capture and thus the sensitivity of ipRGCs (39), although only modest diurnal variation in the excitability of ipRGCs has been reported (223). Resolving this discrepancy will require additional experiments, for instance, to verify functionality of the newly formed melanopsin.

A second form of regulation, seemingly contradictory to the dopamine effect described above, was observed during several days of constant light or darkness. Melanopsin mRNA and protein are dramatically downregulated in constant light and upregulated in constant darkness, even in the absence of signaling from rods and cones (76). Whether this homeostatic regulation of melanopsin expression continues into the long-term is unclear, because mice with degenerated rods/cones have comparable melanopsin levels to wild type (181). Moreover, the PLR of rodless/coneless mice can be summed with that of melanopsin-null mice to account for the wild-type reflex (see above and Ref. 116). Learning the function of this complex, dynamic regulation of melanopsin expression will require further characterization.

Melanopsin expression is also dynamic in nonmammalian vertebrates (4, 29, 67, 93).

VIII. DEVELOPMENT OF INTRINSICALLY PHOTOSENSITIVE RETINAL GANGLION CELLS

IpRGCs are the earliest photoreceptors to appear in development. In mouse, rods and cones become photosensitive on postnatal day 10 (P10). In contrast, ipRGCs are already

photosensitive at birth, showing robust, intrinsically driven Ca^{2+} signals as well as spikes in response to light (Fig. 13*A*) (178, 205). Furthermore, these neonatal ipRGCs appear to be functionally connected to the SCN, as light increases the expression of c-*fos* in this nucleus (74, 119, 178, 222).

Melanopsin is detectable as early as the second week of embryonic development (46, 191), in contrast to rhodopsin, which first appears on P5 (18). Like conventional RGCs, there are many more ipRGCs at birth than in the adult retina. The neonatal density of ipRGCs is ~200 mm^{-2} at birth and drops by 70% to an adult density of ~60 mm^{-2} by P14, corresponding to a couple of days after eye opening (178, but see Ref. 61). Conventional RGCs fall in density by about the same fraction, typically ~50% but reportedly as high as 90% (48). The number of ipRGCs lost in development may be influenced by the presence or absence of the classical photoreceptors (167). The number of ipRGC types is possibly also higher in development, with three physiological types identified in the P8 retina and only two in the adult based on multielectrode-array analysis of sensitivity and spike latency (205).

The sensitivity of ipRGCs increases toward adulthood, up by ~10-fold even just between P4 and P6 (178, 205). IpRGC activity also becomes more sustained (205). This represents a maturation of the intrinsic photosensitivity of the ipRGCs, as these studies were done in retinas without functional rods and cones. Between the first and third postnatal weeks, an additional increase in sensitivity of ipRGCs is observed, consisting of a larger depolarization to light, although there is a faster shut-off as well (Fig. 13*B*) (174). This additional increase in sensitivity is due to maturation of the synaptic drive to ipRGCs, as it is lost with pharmacological block of glutamatergic transmission (174).

The maturation of ipRGCs is evident in their anatomy as well, with the gradual establishment of their adult architecture matching the increase in sensitivity (174, 205). In the first several postnatal days, melanopsin immunolabeling reveals poorly organized ipRGC dendrites in the IPL (205). Two distinct dendritic stratifications are evident in the IPL by P6, and by P19 the dendritic stratifications are well-defined and indistinguishable from adult (205). The size and complexity of the dendritic arbors also increase during development, from a diameter of ~100 μm around birth to ~300 μm by the third postnatal week (174).

As mentioned above, melanopsin is not detectable in the axons of ipRGCs beyond the optic disc (88). Consistent with this finding, melanopsin does not appear to be involved in guiding the ipRGC axons along paths distinct from those of the conventional RGC axons, because the projections of ipRGCs to the brain are normal in *opn4*$^{-/-}$*tau-lacZ*$^{+/+}$ mice (116). The molecular cues that coax the ipRGC axons to their specific targets throughout the brain remain to be identified.

How ipRGCs are specified and whether melanopsin photoreception shapes retinal and brain development in any way are also open questions. Finally, it has been hypothesized that retinal ganglion cells evolved from ancient, rhabdomeric photoreceptors (2). Given that some aspects of phylogeny are reflected in ontogeny (107), it is intriguing that ipRGCs are

the first photoreceptors to appear in development and that melanopsin is a rhabdomeric photopigment (105, 155).

IX. CONCLUSIONS

The ipRGCs constitute a newly discovered channel in mammals for the regulation of physiology and behavior by light. These cells serve the dual function of being intrinsically photosensitive themselves and conveying light information originating from rods and cones. They break an organizational rule in the retina by receiving ON-bipolar cell inputs in the OFF-sublamina of the IPL. IpRGCs distribute light information widely in the brain but also signal locally in the retina, with their influence possibly reaching as far as the rods and cones.

Much remains to be understood, such as the cellular mechanism and the associated molecular constituents of phototransduction, as well as the signal amplification underlying the large single-photon response. Given the diverse functions driven by the ipRGCs, it is likely that there is considerable downstream processing of ipRGC signals. As a precedent, the conventional rod and cone photoreceptors uniformly hyperpolarize to light, but their postsynaptic bipolar cells constitute two broad channels of information: the ON- and OFF-channels (100, 122, 183, 225). The RGCs, postsynaptic to the bipolar cells, have diverse response properties, coding for contrast, directional sensitivity, color, and other even more sophisticated information (5, 59, 121). In the case of the melanopsin system, ipRGCs form synapses in over a dozen brain regions that mediate functions of extreme qualitative and quantitative diversity. For instance, they require only seconds to drive a complete PLR, but tens of minutes or even hours (depending on light intensity) to drive circadian photoentrainment and negative masking. How one molecularly defined population of cells influences such a variety of functions will be a rich area of research.

Last, but not least, the clinical relevance of the ipRGCs has just begun to be explored. Disruption of circadian rhythms has been linked to jet lag, seasonal affective disorder, diabetes, cardiovascular disease, obesity, and even cancer (66, 108, 163, 168, 190). Photoreception during atypical periods may be a factor in some of these disorders (187), and signaling from the ipRGCs themselves has most recently been implicated in an additional pathology, namely, the exacerbation of migraines by light (140). A mutation in melanopsin may be associated with seasonal affective disorder (165), an effective treatment of which is to deliver intense light to the eyes, particularly light enriched in blue, which drives ipRGCs effectively (194). IpRGCs are also compromised in glaucoma (110, 215), a disease that affects circadian rhythms secondary to compromising vision (42). Finally, melanopsin itself has been delivered to the eyes of mice with degenerated rods and cones as one experimental strategy to restore vision (Fig. 14) (111). Thus not only may the study of the melanopsin system yield insights into health and disease, but it may also directly provide tools for therapeutic intervention.

Acknowledgments

GRANTS

This work was funded by National Eye Institute Grant EY-14596 and the Champalimaud Vision Award (to K.-W. Yau).

References

1. Altimus CM, Guler AD, Villa KL, McNeill DS, Legates TA, Hattar S. Rods-cones and melanopsin detect light and dark to modulate sleep independent of image formation. Proc Natl Acad Sci USA. 2008; 105:19998–20003. [PubMed: 19060203]
2. Arendt D, Tessmar-Raible K, Snyman H, Dorresteijn AW, Wittbrodt J. Ciliary photoreceptors with a vertebrate-type opsin in an invertebrate brain. Science. 2004; 306:869–871. [PubMed: 15514158]
3. Bailes HJ, Lucas RJ. Melanopsin and inner retinal photoreception. Cell Mol Life Sci. 2010; 67:99–111. [PubMed: 19865798]
4. Bailey MJ, Cassone VM. Melanopsin expression in the chick retina and pineal gland. Brain Res. 2005; 134:345–348.
5. Barlow HB, Hill RM, Levick WR. Retinal ganglion cells responding selectively to direction and speed of image motion in the rabbit. J Physiol. 1964; 173:377–407. [PubMed: 14220259]
6. Barlow HB, Levick WR. Changes in the maintained discharge with adaptation level in the cat retina. J Physiol. 1969; 202:699–718. [PubMed: 5789945]
7. Barnard AR, Appleford JM, Sekaran S, Chinthapalli K, Jenkins A, Seeliger M, Biel M, Humphries P, Douglas RH, Wenzel A, Foster RG, Hankins MW, Lucas RJ. Residual photosensitivity in mice lacking both rod opsin and cone photoreceptor cyclic nucleotide gated channel 3 alpha subunit. Vis Neurosci. 2004; 21:675–683. [PubMed: 15683556]
8. Barnard AR, Hattar S, Hankins MW, Lucas RJ. Melanopsin regulates visual processing in the mouse retina. Curr Biol. 2006; 16:389–395. [PubMed: 16488873]
9. Baver SB, Pickard GE, Sollars PJ, Pickard GE. Two types of melanopsin retinal ganglion cell differentially innervate the hypo-thalamic suprachiasmatic nucleus and the olivary pretectal nucleus. Eur J Neurosci. 2008; 27:1763–1770. [PubMed: 18371076]
10. Baylor DA, Hodgkin AL, Lamb TD. The electrical response of turtle cones to flashes and steps of light. J Physiol. 1974; 242:685–727. [PubMed: 4449052]
11. Belenky MA, Smeraski CA, Provencio I, Sollars PJ, Pickard GE. Melanopsin retinal ganglion cells receive bipolar and amacrine cell synapses. J Comp Neurol. 2003; 460:380–393. [PubMed: 12692856]
12. Bellingham J, Chaurasia SS, Melyan Z, Liu C, Cameron MA, Tarttelin EE, Iuvone PM, Hankins MW, Tosini G, Lucas RJ. Evolution of melanopsin photoreceptors: discovery and characterization of a new melanopsin in nonmammalian vertebrates. PLoS Biol. 2006; 4:e254. [PubMed: 16856781]
13. Bellingham J, Whitmore D, Philp AR, Wells DJ, Foster RG. Zebrafish melanopsin: isolation, tissue localisation and phylogenetic position. Brain Res. 2002; 107:128–136.
14. Bergstrom AL, Hannibal J, Hindersson P, Fahrenkrug J. Light-induced phase shift in the Syrian hamster (*Mesocricetus auratus*) is attenuated by the PACAP receptor antagonist PACAP6-38 or PACAP immunoneutralization. Eur J Neurosci. 2003; 18:2552–2562. [PubMed: 14622156]
15. Berson DM. Phototransduction in ganglion-cell photoreceptors. Pflügers Arch. 2007; 454:849–855. [PubMed: 17351786]
16. Berson DM, Castrucci AM, Provencio I. Morphology and mosaics of melanopsin-expressing retinal ganglion cell types in mice. J Comp Neurol. 2010; 518:2405–2422. [PubMed: 20503419]
17. Berson DM, Dunn FA, Takao M. Phototransduction by retinal ganglion cells that set the circadian clock. Science. 2002; 295:1070–1073. [PubMed: 11834835]
18. Bibb LC, Holt JK, Tarttelin EE, Hodges MD, Gregory-Evans K, Rutherford A, Lucas RJ, Sowden JC, Gregory-Evans CY. Temporal and spatial expression patterns of the CRX transcription factor and its downstream targets. Critical differences during human and mouse eye development. Hum Mol Genet. 2001; 10:1571–1579. [PubMed: 11468275]
19. Biel M, Seeliger M, Pfeifer A, Kohler K, Gerstner A, Ludwig A, Jaissle G, Fauser S, Zrenner E, Hofmann F. Selective loss of cone function in mice lacking the cyclic nucleotide-gated channel CNG3. Proc Natl Acad Sci USA. 1999; 96:7553–7557. [PubMed: 10377453]

20. Boycott BB, Wassle H. Morphological classification of bipolar cells of the primate retina. Eur J Neurosci. 1991; 3:1069–1088. [PubMed: 12106238]
21. Brainard GC, Sliney D, Hanifin JP, Glickman G, Byrne B, Greeson JM, Jasser S, Gerner E, Rollag MD. Sensitivity of the human circadian system to short-wavelength (420-nm) light. J Biol Rhythms. 2008; 23:379–386. [PubMed: 18838601]
22. Brown TM, Gigg J, Piggins HD, Lucas RJ. Melanopsin-dependent activation of dorsal lateral geniculate neurons. Invest Ophthalmol Vis Sci. 2010; 51:E-Abstract 672.
23. Brown TM, Piggins HD. Electrophysiology of the suprachiasmatic circadian clock. Prog Neurobiol. 2007; 82:229–255. [PubMed: 17646042]
24. Cahill GM, Menaker M. Responses of the suprachiasmatic nucleus to retinohypothalamic tract volleys in a slice preparation of the mouse hypothalamus. Brain Res. 1989; 479:65–75. [PubMed: 2924155]
25. Cahill H, Nathans J. The optokinetic reflex as a tool for quantitative analyses of nervous system function in mice: application to genetic and drug-induced variation. PLoS ONE. 2008; 3:e2055. [PubMed: 18446207]
26. Callaway EM. Transneuronal circuit tracing with neurotropic viruses. Curr Opin Neurobiol. 2008; 18:617–623. [PubMed: 19349161]
27. Calvert PD, Krasnoperova NV, Lyubarsky AL, Isayama T, Nicolo M, Kosaras B, Wong G, Gannon KS, Margolskee RF, Sidman RL, Pugh EN Jr, Makino CL, Lem J. Phototransduction in transgenic mice after targeted deletion of the rod transducin alpha-subunit. Proc Natl Acad Sci USA. 2000; 97:13913–13918. [PubMed: 11095744]
28. Cameron MA, Pozdeyev N, Vugler AA, Cooper H, Iuvone PM, Lucas RJ. Light regulation of retinal dopamine that is independent of melanopsin phototransduction. Eur J Neurosci. 2009; 29:761–767. [PubMed: 19200071]
29. Chaurasia SS, Rollag MD, Jiang G, Hayes WP, Haque R, Natesan A, Zatz M, Tosini G, Liu C, Korf HW, Iuvone PM, Provencio I. Molecular cloning, localization and circadian expression of chicken melanopsin (*Opn4*): differential regulation of expression in pineal and retinal cell types. J Neurochem. 2005; 92:158–170. [PubMed: 15606905]
30. Cheng N, Tsunenari T, Yau KW. Intrinsic light response of retinal horizontal cells of teleosts. Nature. 2009; 460:899–903. [PubMed: 19633653]
31. Colwell CS, Michel S, Itri J, Rodriguez W, Tam J, Lelievre V, Hu Z, Waschek JA. Selective deficits in the circadian light response in mice lacking PACAP. Am J Physiol Regul Integr Comp Physiol. 2004; 287:R1194–R1201. [PubMed: 15217792]
32. Contin MA, Verra DM, Guido ME. An invertebrate-like phototransduction cascade mediates light detection in the chicken retinal ganglion cells. FASEB J. 2006; 20:2648–2650. [PubMed: 17077288]
33. Contini M, Raviola E. GABAergic synapses made by a retinal dopaminergic neuron. Proc Natl Acad Sci USA. 2003; 100:1358–1363. [PubMed: 12547914]
34. Czeisler CA, Shanahan TL, Klerman EB, Martens H, Brotman DJ, Emens JS, Klein T, Rizzo JF 3rd. Suppression of melatonin secretion in some blind patients by exposure to bright light. N Engl J Med. 1995; 332:6–11. [PubMed: 7990870]
35. Dacey DM, Liao HW, Peterson BB, Robinson FR, Smith VC, Pokorny J, Yau KW, Gamlin PD. Melanopsin-expressing ganglion cells in primate retina signal colour and irradiance and project to the LGN. Nature. 2005; 433:749–754. [PubMed: 15716953]
36. Dacey DM, Peterson BB, Liao HW, Yau KW. Two types of melanopsin-containing ganglion cells in the primate retina: links to dopaminergic amacrine and DB6 cone bipolar cells. Invest Ophthalmol Vis Sci. 2006; 47:E-Abstract 3111.
37. Dkhissi-Benyahya O, Rieux C, Hut RA, Cooper HM. Immunohistochemical evidence of a melanopsin cone in human retina. Invest Ophthalmol Vis Sci. 2006; 47:1636–1641. [PubMed: 16565403]
38. Do MTH, Bean BP. Subthreshold sodium currents and pacemaking of subthalamic neurons: modulation by slow inactivation. Neuron. 2003; 39:109–120. [PubMed: 12848936]
39. Do MTH, Kang SH, Xue T, Zhong H, Liao HW, Bergles DE, Yau KW. Photon capture and signalling by melanopsin retinal ganglion cells. Nature. 2009; 457:281–287. [PubMed: 19118382]

40. Doyle SE, Castrucci AM, McCall M, Provencio I, Menaker M. Nonvisual light responses in the Rpe65 knockout mouse: rod loss restores sensitivity to the melanopsin system. Proc Natl Acad Sci USA. 2006; 103:10432–10437. [PubMed: 16788070]
41. Drivenes O, Soviknes AM, Ebbesson LO, Fjose A, Seo HC, Helvik JV. Isolation and characterization of two teleost melanopsin genes and their differential expression within the inner retina and brain. J Comp Neurol. 2003; 456:84–93. [PubMed: 12508316]
42. Drouyer E, Dkhissi-Benyahya O, Chiquet C, WoldeMussie E, Ruiz G, Wheeler LA, Denis P, Cooper HM. Glaucoma alters the circadian timing system. PLoS ONE. 2008; 3:e3931. [PubMed: 19079596]
43. Dumitrescu ON, Pucci FG, Wong KY, Berson DM. Ectopic retinal ON bipolar cell synapses in the OFF inner plexiform layer: contacts with dopaminergic amacrine cells and melanopsin ganglion cells. J Comp Neurol. 2009; 517:226–244. [PubMed: 19731338]
44. Euler T, Wassle H. Immunocytochemical identification of cone bipolar cells in the rat retina. J Comp Neurol. 1995; 361:461–478. [PubMed: 8550893]
45. Fahrenkrug J, Falktoft B, Georg B, Rask L. *N*-linked deglycosylated melanopsin retains its responsiveness to light. Biochemistry. 2009; 48:5142–5148. [PubMed: 19413349]
46. Fahrenkrug J, Nielsen HS, Hannibal J. Expression of melanopsin during development of the rat retina. Neuroreport. 2004; 15:781–784. [PubMed: 15073514]
47. Fain GL, Hardie R, Laughlin SB. Phototransduction and the evolution of photoreceptors. Curr Biol. 2010; 20:R114–124. [PubMed: 20144772]
48. Farah MH. Neurogenesis and cell death in the ganglion cell layer of vertebrate retina. Brain Res Rev. 2006; 52:264–274. [PubMed: 16764935]
49. Feigenspan A, Gustincich S, Bean BP, Raviola E. Spontaneous activity of solitary dopaminergic cells of the retina. J Neurosci. 1998; 18:6776–6789. [PubMed: 9712649]
50. Field GD, Sampath AP, Rieke F. Retinal processing near absolute threshold: from behavior to mechanism. Annu Rev Physiol. 2005; 67:491–514. [PubMed: 15709967]
51. Foster RG, Provencio I, Hudson D, Fiske S, De Grip W, Menaker M. Circadian photoreception in the retinally degenerate mouse (*rd*/*rd*). J Comp Physiol A Sens Neural Behav Physiol. 1991; 169:39–50.
52. Freedman MS, Lucas RJ, Soni B, von Schantz M, Munoz M, David-Gray Z, Foster R. Regulation of mammalian circadian behavior by non-rod, non-cone, and ocular photoreceptors. Science. 1999; 284:502–504. [PubMed: 10205061]
53. Frigato E, Vallone D, Bertolucci C, Foulkes NS. Isolation and characterization of melanopsin and pinopsin expression within photoreceptive sites of reptiles. Naturwissenschaften. 2006; 93:379–385. [PubMed: 16688437]
54. Fu Y, Liao HW, Do MTH, Yau KW. Non-image-forming ocular photoreception in vertebrates. Curr Opin Neurobiol. 2005; 15:415–422. [PubMed: 16023851]
55. Fu Y, Zhong H, Wang MH, Luo DG, Liao HW, Maeda H, Hattar S, Frishman LJ, Yau KW. Intrinsically photosensitive retinal ganglion cells detect light with a vitamin A-based photopigment, melanopsin. Proc Natl Acad Sci USA. 2005; 102:10339–10344. [PubMed: 16014418]
56. Gamlin PD, McDougal DH, Pokorny J, Smith VC, Yau KW, Dacey DM. Human and macaque pupil responses driven by melanopsin-containing retinal ganglion cells. Vision Res. 2007; 47:946–954. [PubMed: 17320141]
57. Ghosh KK, Bujan S, Haverkamp S, Feigenspan A, Wassle H. Types of bipolar cells in the mouse retina. J Comp Neurol. 2004; 469:70–82. [PubMed: 14689473]
58. Giesbers ME, Shirzad-Wasei N, Bosman GJ, de Grip WJ. Functional expression, targeting and Ca^{2+} signaling of a mouse melanopsin-eYFP fusion protein in a retinal pigment epithelium cell line. Photochem Photobiol. 2008; 84:990–995. [PubMed: 18422879]
59. Gollisch T, Meister M. Eye smarter than scientists believed: neural computations in circuits of the retina. Neuron. 2010; 65:150–164. [PubMed: 20152123]
60. del Pilar Gomez M, Angueyra JM, Nasi E. Light-transduction in melanopsin-expressing photoreceptors of *Amphioxus*. Proc Natl Acad Sci USA. 2009; 106:9081–9086. [PubMed: 19451628]

61. Gonzalez-Menendez I, Contreras F, Cernuda-Cernuda R, Garcia-Fernandez JM. No loss of melanopsin-expressing ganglion cells detected during postnatal development of the mouse retina. Histol Histopathol. 25:73–82. [PubMed: 19924643]

62. Gooley JJ, Lu J, Chou TC, Scammell TE, Saper CB. Melanopsin in cells of origin of the retinohypothalamic tract. Nat Neurosci. 2001; 4:1165. [PubMed: 11713469]

63. Gooley JJ, Lu J, Fischer D, Saper CB. A broad role for melanopsin in nonvisual photoreception. J Neurosci. 2003; 23:7093–7106. [PubMed: 12904470]

64. Goz D, Studholme K, Lappi DA, Rollag MD, Provencio I, Morin LP. Targeted destruction of photosensitive retinal ganglion cells with a saporin conjugate alters the effects of light on mouse circadian rhythms. PLoS ONE. 2008; 3:e3153. [PubMed: 18773079]

65. Graham DM, Wong KY, Shapiro P, Frederick C, Pattabiraman K, Berson DM. Melanopsin ganglion cells use a membrane-associated rhabdomeric phototransduction cascade. J Neurophysiol. 2008; 99:2522–2532. [PubMed: 18305089]

66. Green CB, Takahashi JS, Bass J. The meter of metabolism. Cell. 2008; 134:728–742. [PubMed: 18775307]

67. Grone BP, Sheng Z, Chen CC, Fernald RD. Localization and diurnal expression of melanopsin, vertebrate ancient opsin, and pituitary adenylate cyclase-activating peptide mRNA in a teleost retina. J Biol Rhythms. 2007; 22:558–561. [PubMed: 18057331]

68. Grozdanic SD, Matic M, Sakaguchi DS, Kardon RH. Evaluation of retinal status using chromatic pupil light reflex activity in healthy and diseased canine eyes. Invest Ophthalmol Vis Sci. 2007; 48:5178–5183. [PubMed: 17962471]

69. Guldner FH. Synapses of optic nerve afferents in the rat supra-chiasmatic nucleus. I. Identification, qualitative description, development and distribution. Cell Tissue Res. 1978; 194:17–35. [PubMed: 719729]

70. Guler AD, Ecker JL, Lall GS, Haq S, Altimus CM, Liao HW, Barnard AR, Cahill H, Badea TC, Zhao H, Hankins MW, Berson DM, Lucas RJ, Yau KW, Hattar S. Melanopsin cells are the principal conduits for rod-cone input to non-image-forming vision. Nature. 2008; 453:102–105. [PubMed: 18432195]

71. Hankins MW, Lucas RJ. The primary visual pathway in humans is regulated according to long-term light exposure through the action of a nonclassical photopigment. Curr Biol. 2002; 12:191–198. [PubMed: 11839270]

72. Hankins MW, Peirson SN, Foster RG. Melanopsin: an exciting photopigment. Trends Neurosci. 2008; 31:27–36. [PubMed: 18054803]

73. Hannibal J. Roles of PACAP-containing retinal ganglion cells in circadian timing. Int Rev Cytol. 2006; 251:1–39. [PubMed: 16939776]

74. Hannibal J, Fahrenkrug J. Melanopsin containing retinal ganglion cells are light responsive from birth. Neuroreport. 2004; 15:2317–2320. [PubMed: 15640747]

75. Hannibal J, Fahrenkrug J. Target areas innervated by PACAP-immunoreactive retinal ganglion cells. Cell Tissue Res. 2004; 316:99–113. [PubMed: 14991397]

76. Hannibal J, Georg B, Hindersson P, Fahrenkrug J. Light and darkness regulate melanopsin in the retinal ganglion cells of the albino Wistar rat. J Mol Neurosci. 2005; 27:147–155. [PubMed: 16186625]

77. Hannibal J, Hindersson P, Knudsen SM, Georg B, Fahrenkrug J. The photopigment melanopsin is exclusively present in pituitary adenylate cyclase-activating polypeptide-containing retinal ganglion cells of the retinohypothalamic tract. J Neurosci. 2002; 22:RC191. [PubMed: 11756521]

78. Hannibal J, Hindersson P, Nevo E, Fahrenkrug J. The circadian photopigment melanopsin is expressed in the blind subterranean mole rat, *Spalax*. Neuroreport. 2002; 13:1411–1414. [PubMed: 12167764]

79. Hannibal J, Hindersson P, Ostergaard J, Georg B, Heegaard S, Larsen PJ, Fahrenkrug J. Melanopsin is expressed in PACAP-containing retinal ganglion cells of the human retinohypothalamic tract. Invest Ophthalmol Vis Sci. 2004; 45:4202–4209. [PubMed: 15505076]

80. Hardie, RC.; Postma, M. Phototransduction in microvillar photoreceptors of *Drosophila* and other invertebrates. In: Basbaum, AI., editor. The Senses: A Comprehensive Reference. New York: Elsevier Science/Academic Press; 2008.

81. Harmar AJ. An essential role for peptidergic signalling in the control of circadian rhythms in the suprachiasmatic nuclei. J Neuroendocrinol. 2003; 15:335–338. [PubMed: 12622830]

82. Hartline HK. Intensity and duration in the excitation of single photoreceptor units. J Cell Comp Physiol. 1934; 5:229–247.

83. Hartwick AT, Bramley JR, Yu J, Stevens KT, Allen CN, Baldridge WH, Sollars PJ, Pickard GE. Light-evoked calcium responses of isolated melanopsin-expressing retinal ganglion cells. J Neurosci. 2007; 27:13468–13480. [PubMed: 18057205]

84. Hashimoto H, Shintani N, Baba A. New insights into the central PACAPergic system from the phenotypes in PACAP- and PACAP receptor-knockout mice. Ann NY Acad Sci. 2006; 1070:75–89. [PubMed: 16888150]

85. Hatori M, Le H, Vollmers C, Keding SR, Tanaka N, Schmedt C, Jegla T, Panda S. Inducible ablation of melanopsin-expressing retinal ganglion cells reveals their central role in non-image forming visual responses. PLoS ONE. 2008; 3:e2451. [PubMed: 18545654]

86. Hattar S, Ecker JL, Dumitrescu ON, Chen SK, Wong KY, Alam NM, Prusky GT, Berson DM. Functions and target innervations of distinct subtypes of melanopsin cells. Invest Ophthalmol Vis Sci. 2009; 50:E-Abstract 5027.

87. Hattar S, Kumar M, Park A, Tong P, Tung J, Yau KW, Berson DM. Central projections of melanopsin-expressing retinal ganglion cells in the mouse. J Comp Neurol. 2006; 497:326–349. [PubMed: 16736474]

88. Hattar S, Liao HW, Takao M, Berson DM, Yau KW. Melanopsin-containing retinal ganglion cells: architecture, projections, and intrinsic photosensitivity. Science. 2002; 295:1065–1070. [PubMed: 11834834]

89. Hattar S, Lucas RJ, Mrosovsky N, Thompson S, Douglas RH, Hankins MW, Lem J, Biel M, Hofmann F, Foster RG, Yau KW. Melanopsin and rod-cone photoreceptive systems account for all major accessory visual functions in mice. Nature. 2003; 424:76–81. [PubMed: 12808468]

90. Hecht S, Shlaer S, Pirenne MH. Energy, quanta, and vision. J Gen Physiol. 1942; 25:819–840. [PubMed: 19873316]

91. Hillman P, Hochstein S, Minke B. Transduction in invertebrate photoreceptors: role of pigment bistability. Physiol Rev. 1983; 63:668–772. [PubMed: 6340134]

92. Hokoc JN, Mariani AP. Tyrosine hydroxylase immunoreactivity in the rhesus monkey retina reveals synapses from bipolar cells to dopaminergic amacrine cells. J Neurosci. 1987; 7:2785–2793. [PubMed: 2887643]

93. Holthues H, Engel L, Spessert R, Vollrath L. Circadian gene expression patterns of melanopsin and pinopsin in the chick pineal gland. Biochem Biophys Res Commun. 2005; 326:160–165. [PubMed: 15567166]

94. Hoshi H, Liu WL, Massey SC, Mills SL. ON inputs to the OFF layer: bipolar cells that break the stratification rules of the retina. J Neurosci. 2009; 29:8875–8883. [PubMed: 19605625]

95. Ingham ES, Gunhan E, Fuller PM, Fuller CA. Immunotoxin-induced ablation of melanopsin retinal ganglion cells in a non-murine mammalian model. J Comp Neurol. 2009; 516:125–140. [PubMed: 19575450]

96. Isoldi MC, Rollag MD, Castrucci AM, Provencio I. Rhabdomeric phototransduction initiated by the vertebrate photopigment melanopsin. Proc Natl Acad Sci USA. 2005; 102:1217–1221. [PubMed: 15653769]

97. Jackson AC, Yao GL, Bean BP. Mechanism of spontaneous firing in dorsomedial suprachiasmatic nucleus neurons. J Neurosci. 2004; 24:7985–7998. [PubMed: 15371499]

98. Jenkins A, Munoz M, Tarttelin EE, Bellingham J, Foster RG, Hankins MW. VA opsin, melanopsin, and an inherent light response within retinal interneurons. Curr Biol. 2003; 13:1269–1278. [PubMed: 12906786]

99. Jusuf PR, Lee SC, Hannibal J, Grunert U. Characterization and synaptic connectivity of melanopsin-containing ganglion cells in the primate retina. Eur J Neurosci. 2007; 26:2906–2921. [PubMed: 18001286]

100. Kaneko A. Physiological and morphological identification of horizontal, bipolar and amacrine cells in goldfish retina. J Physiol. 1970; 207:623–633. [PubMed: 5499739]

101. Kardon R, Anderson SC, Damarjian TG, Grace EM, Stone E, Kawasaki A. Chromatic pupil responses preferential activation of the melanopsin-mediated versus outer photoreceptor-mediated pupil light reflex. Ophthalmology. 2009; 116:1564–1573. [PubMed: 19501408]
102. Kim YI, Dudek FE. Intracellular electrophysiological study of suprachiasmatic nucleus neurons in rodents: excitatory synaptic mechanisms. J Physiol. 1991; 444:269–287. [PubMed: 1688029]
103. Klerman EB, Shanahan TL, Brotman DJ, Rimmer DW, Emens JS, Rizzo JF 3rd, Czeisler CA. Photic resetting of the human circadian pacemaker in the absence of conscious vision. J Biol Rhythms. 2002; 17:548–555. [PubMed: 12465888]
104. Kosaka T, Kosaka K, Hataguchi Y, Nagatsu I, Wu JY, Ottersen OP, Storm-Mathisen J, Hama K. Catecholaminergic neurons containing GABA-like and/or glutamic acid decarboxylase-like immunoreactivities in various brain regions of the rat. Exp Brain Res. 1987; 66:191–210. [PubMed: 2884126]
105. Koyanagi M, Kubokawa K, Tsukamoto H, Shichida Y, Terakita A. Cephalochordate melanopsin: evolutionary linkage between invertebrate visual cells and vertebrate photosensitive retinal ganglion cells. Curr Biol. 2005; 15:1065–1069. [PubMed: 15936279]
106. Kumbalasiri T, Provencio I. Melanopsin and other novel mammalian opsins. Exp Eye Res. 2005; 81:368–375. [PubMed: 16005867]
107. Lamb TD, Collin SP, Pugh EN Jr. Evolution of the vertebrate eye: opsins, photoreceptors, retina and eye cup. Nat Rev Neurosci. 2007; 8:960–976. [PubMed: 18026166]
108. Laposky AD, Bass J, Kohsaka A, Turek FW. Sleep and circadian rhythms: key components in the regulation of energy metabolism. FEBS Lett. 2008; 582:142–151. [PubMed: 17707819]
109. Lem J, Krasnoperova NV, Calvert PD, Kosaras B, Cameron DA, Nicolo M, Makino CL, Sidman RL. Morphological, physiological, and biochemical changes in rhodopsin knockout mice. Proc Natl Acad Sci USA. 1999; 96:736–741. [PubMed: 9892703]
110. Li RS, Chen BY, Tay DK, Chan HH, Pu ML, So KF. Melanopsin-expressing retinal ganglion cells are more injury-resistant in a chronic ocular hypertension model. Invest Ophthalmol Vis Sci. 2006; 47:2951–2958. [PubMed: 16799038]
111. Lin B, Koizumi A, Tanaka N, Panda S, Masland RH. Restoration of visual function in retinal degeneration mice by ectopic expression of melanopsin. Proc Natl Acad Sci USA. 2008; 105:16009–16014. [PubMed: 18836071]
112. Lockley SW, Brainard GC, Czeisler CA. High sensitivity of the human circadian melatonin rhythm to resetting by short wavelength light. J Clin Endocrinol Metab. 2003; 88:4502–4505. [PubMed: 12970330]
113. Lucas RJ, Douglas RH, Foster RG. Characterization of an ocular photopigment capable of driving pupillary constriction in mice. Nat Neurosci. 2001; 4:621–626. [PubMed: 11369943]
114. Lucas RJ, Foster RG. Neither functional rod photoreceptors nor rod or cone outer segments are required for the photic inhibition of pineal melatonin. Endocrinology. 1999; 140:1520–1524. [PubMed: 10098483]
115. Lucas RJ, Freedman MS, Munoz M, Garcia-Fernandez JM, Foster RG. Regulation of the mammalian pineal by non-rod, non-cone, and ocular photoreceptors. Science. 1999; 284:505–507. [PubMed: 10205062]
116. Lucas RJ, Hattar S, Takao M, Berson DM, Foster RG, Yau KW. Diminished pupillary light reflex at high irradiances in melanopsin-knockout mice. Science. 2003; 299:245–247. [PubMed: 12522249]
117. Luo, DG.; Kefalov, V.; Yau, KW. Phototransduction in retinal rods and cones. In: Basbaum, AI., editor. The Senses: A Comprehensive Reference. New York: Elsevier/Academic; 2008.
118. Lupi D, Oster H, Thompson S, Foster RG. The acute light-induction of sleep is mediated by *OPN4*-based photoreception. Nat Neurosci. 2008; 11:1068–1073. [PubMed: 19160505]
119. Lupi D, Sekaran S, Jones SL, Hankins MW, Foster RG. Light-evoked FOS induction within the suprachiasmatic nuclei (SCN) of melanopsin knockout (*Opn4*$^{-/-}$) mice: a developmental study. Chronobiol Int. 2006; 23:167–179. [PubMed: 16687291]
120. Mariani AP. Giant bistratified bipolar cells in monkey retina. Anat Rec. 1983; 206:215–220.
121. Masland RH. The fundamental plan of the retina. Nat Neurosci. 2001; 4:877–886. [PubMed: 11528418]

122. Masu M, Iwakabe H, Tagawa Y, Miyoshi T, Yamashita M, Fukuda Y, Sasaki H, Hiroi K, Nakamura Y, Shigemoto R. Specific deficit of the ON response in visual transmission by targeted disruption of the mGluR6 gene. Cell. 1995; 80:757–765. [PubMed: 7889569]

123. Mathes A, Engel L, Holthues H, Wolloscheck T, Spessert R. Daily profile in melanopsin transcripts depends on seasonal lighting conditions in the rat retina. J Neuroendocrinol. 2007; 19:952–957. [PubMed: 18001324]

124. Mawad K, Van Gelder RN. Absence of long-wavelength photic potentiation of murine intrinsically photosensitive retinal ganglion cell firing in vitro. J Biol Rhythms. 2008; 23:387–391. [PubMed: 18838602]

125. McCall MA, Gregg RG, Merriman K, Goto Y, Peachey NS, Stanford LR. Morphological and physiological consequences of the selective elimination of rod photoreceptors in transgenic mice. Exp Eye Res. 1996; 63:35–50. [PubMed: 8983962]

126. McDougal DH, Gamlin PD. The influence of intrinsically-photosensitive retinal ganglion cells on the spectral sensitivity and response dynamics of the human pupillary light reflex. Vision Res. 2010; 50:72–87. [PubMed: 19850061]

127. Melyan Z, Tarttelin EE, Bellingham J, Lucas RJ, Hankins MW. Addition of human melanopsin renders mammalian cells photoresponsive. Nature. 2005; 433:741–745. [PubMed: 15674244]

128. Meyer-Arendt JR. Radiometry and photometry: units and conversion factors. Appl Opt. 1968; 7:2081. [PubMed: 20068937]

129. Morgan WW, Kamp CW. Dopaminergic amacrine neurons of rat retinas with photoreceptor degeneration continue to respond to light. Life Sci. 1980; 26:1619–1626. [PubMed: 7382733]

130. Morin LP, Blanchard JH, Provencio I. Retinal ganglion cell projections to the hamster suprachiasmatic nucleus, intergeniculate leaflet, and visual midbrain: bifurcation and melanopsin immunoreactivity. J Comp Neurol. 2003; 465:401–416. [PubMed: 12966564]

131. Mrosovsky N. Further characterization of the phenotype of mCry1/mCry2-deficient mice. Chronobiol Int. 2001; 18:613–625. [PubMed: 11587085]

132. Mrosovsky N. Masking: history, definitions, and measurement. Chronobiol Int. 1999; 16:415–429. [PubMed: 10442236]

133. Mrosovsky N, Hattar S. Impaired masking responses to light in melanopsin-knockout mice. Chronobiol Int. 2003; 20:989–999. [PubMed: 14680139]

134. Mure LS, Cornut PL, Rieux C, Drouyer E, Denis P, Gronfier C, Cooper HM. Melanopsin bistability: a fly's eye technology in the human retina. PLoS ONE. 2009; 4:e5991. [PubMed: 19551136]

135. Mure LS, Rieux C, Hattar S, Cooper HM. Melanopsin-dependent nonvisual responses: evidence for photopigment bistability in vivo. J Biol Rhythms. 2007; 22:411–424. [PubMed: 17876062]

136. Nayak SK, Jegla T, Panda S. Role of a novel photopigment, melanopsin, in behavioral adaptation to light. Cell Mol Life Sci. 2007; 64:144–154. [PubMed: 17160354]

137. Nelson DE, Takahashi JS. Sensitivity and integration in a visual pathway for circadian entrainment in the hamster (*Mesocricetus auratus*). J Physiol. 1991; 439:115–145. [PubMed: 1895235]

138. Newman EA. Glial modulation of synaptic transmission in the retina. Glia. 2004; 47:268–274. [PubMed: 15252816]

139. Newman LA, Walker MT, Brown RL, Cronin TW, Robinson PR. Melanopsin forms a functional short-wavelength photopigment. Biochemistry. 2003; 42:12734–12738. [PubMed: 14596587]

140. Noseda R, Kainz V, Jakubowski M, Gooley JJ, Saper CB, Digre K, Burstein R. A neural mechanism for exacerbation of headache by light. Nat Neurosci. 2010; 13:239–245. [PubMed: 20062053]

141. Ogden TE, Miller RF. Studies of the optic nerve of the rhesus monkey: nerve fiber spectrum and physiological properties. Vision Res. 1966; 6:485–506. [PubMed: 4976686]

142. Ostergaard J, Hannibal J, Fahrenkrug J. Synaptic contact between melanopsin-containing retinal ganglion cells and rod bipolar cells. Invest Ophthalmol Vis Sci. 2007; 48:3812–3820. [PubMed: 17652756]

143. Panda S, Nayak SK, Campo B, Walker JR, Hogenesch JB, Jegla T. Illumination of the melanopsin signaling pathway. Science. 2005; 307:600–604. [PubMed: 15681390]

144. Panda S, Provencio I, Tu DC, Pires SS, Rollag MD, Castrucci AM, Pletcher MT, Sato TK, Wiltshire T, Andahazy M, Kay SA, Van Gelder RN, Hogenesch JB. Melanopsin is required for non-image-forming photic responses in blind mice. Science. 2003; 301:525–527. [PubMed: 12829787]

145. Panda S, Sato TK, Castrucci AM, Rollag MD, DeGrip WJ, Hogenesch JB, Provencio I, Kay SA. Melanopsin (*Opn4*) requirement for normal light-induced circadian phase shifting. Science. 2002; 298:2213–2216. [PubMed: 12481141]

146. Parnas M, Katz B, Lev S, Tzarfaty V, Dadon D, Gordon-Shaag A, Metzner H, Yaka R, Minke B. Membrane lipid modulations remove divalent open channel block from TRP-like and NMDA channels. J Neurosci. 2009; 29:2371–2383. [PubMed: 19244513]

147. Peirson SN, Bovee-Geurts PH, Lupi D, Jeffery G, DeGrip WJ, Foster RG. Expression of the candidate circadian photopigment melanopsin (*Opn4*) in the mouse retinal pigment epithelium. Brain Res. 2004; 123:132–135.

148. Peirson SN, Oster H, Jones SL, Leitges M, Hankins MW, Foster RG. Microarray analysis and functional genomics identify novel components of melanopsin signaling. Curr Biol. 2007; 17:1363–1372. [PubMed: 17702581]

149. Perez-Leon JA, Warren EJ, Allen CN, Robinson DW, Lane Brown R. Synaptic inputs to retinal ganglion cells that set the circadian clock. Eur J Neurosci. 2006; 24:1117–1123. [PubMed: 16930437]

150. Pickard GE, Baver SB, Ogilvie MD, Sollars PJ. Light-induced fos expression in intrinsically photosensitive retinal ganglion cells in melanopsin knockout (*Opn4*) mice. PLoS ONE. 2009; 4:e4984. [PubMed: 19319185]

151. Pickard GE, Smeraski CA, Tomlinson CC, Banfield BW, Kaufman J, Wilcox CL, Enquist LW, Sollars PJ. Intravitreal injection of the attenuated pseudorabies virus PRV Bartha results in infection of the hamster suprachiasmatic nucleus only by retrograde transsynaptic transport via autonomic circuits. J Neurosci. 2002; 22:2701–2710. [PubMed: 11923435]

152. Pires SS, Hughes S, Turton M, Melyan Z, Peirson SN, Zheng L, Kosmaoglou M, Bellingham J, Cheetham ME, Lucas RJ, Foster RG, Hankins MW, Halford S. Differential expression of two distinct functional isoforms of melanopsin (*Opn4*) in the mammalian retina. J Neurosci. 2009; 29:12332–12342. [PubMed: 19793992]

153. Pires SS, Shand J, Bellingham J, Arrese C, Turton M, Peirson S, Foster RG, Halford S. Isolation and characterization of melanopsin (*Opn4*) from the Australian marsupial *Sminthopsis crassicaudata* (fat-tailed dunnart). Proc Biol Sci. 2007; 274:2791–2799. [PubMed: 17785267]

154. Provencio I, Foster RG. Circadian rhythms in mice can be regulated by photoreceptors with cone-like characteristics. Brain Res. 1995; 694:183–190. [PubMed: 8974643]

155. Provencio I, Jiang G, De Grip WJ, Hayes WP, Rollag MD. Melanopsin: an opsin in melanophores, brain, and eye. Proc Natl Acad Sci USA. 1998; 95:340–345. [PubMed: 9419377]

156. Provencio I, Rodriguez IR, Jiang G, Hayes WP, Moreira EF, Rollag MD. A novel human opsin in the inner retina. J Neurosci. 2000; 20:600–605. [PubMed: 10632589]

157. Provencio I, Rollag MD, Castrucci AM. Photoreceptive net in the mammalian retina. This mesh of cells may explain how some blind mice can still tell day from night. Nature. 2002; 415:493. [PubMed: 11823848]

158. Provencio I, Wong S, Lederman AB, Argamaso SM, Foster RG. Visual and circadian responses to light in aged retinally degenerate mice. Vision Res. 1994; 34:1799–1806. [PubMed: 7941382]

159. Pu M. Physiological response properties of cat retinal ganglion cells projecting to suprachiasmatic nucleus. J Biol Rhythms. 2000; 15:31–36. [PubMed: 10677014]

160. Qiu X, Berson DM. Melanopsin bistability in ganglion-cell photoreceptors. Invest Ophthalmol Vis Sci. 2007; 48:E-Abstract 612.

161. Qiu X, Kumbalasiri T, Carlson SM, Wong KY, Krishna V, Provencio I, Berson DM. Induction of photosensitivity by heterologous expression of melanopsin. Nature. 2005; 433:745–749. [PubMed: 15674243]

162. Ramsey IS, Delling M, Clapham DE. An introduction to TRP channels. Annu Rev Physiol. 2006; 68:619–647. [PubMed: 16460286]

163. Reid KJ, Zee PC. Circadian rhythm disorders. Semin Neurol. 2009; 29:393–405. [PubMed: 19742414]

164. Rieke F, Rudd ME. The challenges natural images pose for visual adaptation. Neuron. 2009; 64:605–616. [PubMed: 20005818]

165. Roecklein KA, Rohan KJ, Duncan WC, Rollag MD, Rosenthal NE, Lipsky RH, Provencio I. A missense variant (P10L) of the melanopsin (*OPN4*) gene in seasonal affective disorder. J Affect Disord. 2009; 114:279–285. [PubMed: 18804284]

166. Ruby NF, Brennan TJ, Xie X, Cao V, Franken P, Heller HC, O'Hara BF. Role of melanopsin in circadian responses to light. Science. 2002; 298:2211–2213. [PubMed: 12481140]

167. Ruggiero L, Allen CN, Lane Brown R, Robinson DW. The development of melanopsin-containing retinal ganglion cells in mice with early retinal degeneration. Eur J Neurosci. 2009; 29:359–367. [PubMed: 19200239]

168. Sahar S, Sassone-Corsi P. Metabolism and cancer: the circadian clock connection. Nat Rev Cancer. 2009; 9:886–896. [PubMed: 19935677]

169. Sakamoto K, Liu C, Kasamatsu M, Pozdeyev NV, Iuvone PM, Tosini G. Dopamine regulates melanopsin mRNA expression in intrinsically photosensitive retinal ganglion cells. Eur J Neurosci. 2005; 22:3129–3136. [PubMed: 16367779]

170. Sakamoto K, Liu C, Tosini G. Classical photoreceptors regulate melanopsin mRNA levels in the rat retina. J Neurosci. 2004; 24:9693–9697. [PubMed: 15509757]

171. Sampath AP, Rieke F. Selective transmission of single photon responses by saturation at the rod-to-rod bipolar synapse. Neuron. 2004; 41:431–443. [PubMed: 14766181]

172. Saper CB, Cano G, Scammell TE. Homeostatic, circadian, and emotional regulation of sleep. J Comp Neurol. 2005; 493:92–98. [PubMed: 16254994]

173. Schmidt TM, Kofuji P. Functional and morphological differences among intrinsically photosensitive retinal ganglion cells. J Neurosci. 2009; 29:476–482. [PubMed: 19144848]

174. Schmidt TM, Taniguchi K, Kofuji P. Intrinsic and extrinsic light responses in melanopsin-expressing ganglion cells during mouse development. J Neurophysiol. 2008; 100:371–384. [PubMed: 18480363]

175. Schmucker C, Seeliger M, Humphries P, Biel M, Schaeffel F. Grating acuity at different luminances in wild-type mice and in mice lacking rod or cone function. Invest Ophthalmol Vis Sci. 2005; 46:398–407. [PubMed: 15623801]

176. Sekaran S, Foster RG, Lucas RJ, Hankins MW. Calcium imaging reveals a network of intrinsically light-sensitive inner-retinal neurons. Curr Biol. 2003; 13:1290–1298. [PubMed: 12906788]

177. Sekaran S, Lall GS, Ralphs KL, Wolstenholme AJ, Lucas RJ, Foster RG, Hankins MW. 2-Aminoethoxydiphenylborane is an acute inhibitor of directly photosensitive retinal ganglion cell activity in vitro and in vivo. J Neurosci. 2007; 27:3981–3986. [PubMed: 17428972]

178. Sekaran S, Lupi D, Jones SL, Sheely CJ, Hattar S, Yau KW, Lucas RJ, Foster RG, Hankins MW. Melanopsin-dependent photoreception provides earliest light detection in the mammalian retina. Curr Biol. 2005; 15:1099–1107. [PubMed: 15964274]

179. Selby CP, Thompson C, Schmitz TM, Van Gelder RN, Sancar A. Functional redundancy of cryptochromes and classical photoreceptors for nonvisual ocular photoreception in mice. Proc Natl Acad Sci USA. 2000; 97:14697–14702. [PubMed: 11114194]

180. Semo M, Munoz Llamosas M, Foster RG, Jeffery G. Melanopsin (*Opn4*) positive cells in the cat retina are randomly distributed across the ganglion cell layer. Vis Neurosci. 2005; 22:111–116. [PubMed: 15842746]

181. Semo M, Peirson S, Lupi D, Lucas RJ, Jeffery G, Foster RG. Melanopsin retinal ganglion cells and the maintenance of circadian and pupillary responses to light in aged rodless/coneless (*rd/rd cl*) mice. Eur J Neurosci. 2003; 17:1793–1801. [PubMed: 12752778]

182. Silva MM, Albuquerque AM, Araujo JF. Light-dark cycle synchronization of circadian rhythm in blind primates. J Circadian Rhythms. 2005; 3:10. [PubMed: 16144547]

183. Slaughter MM, Miller RF. 2-Amino-4-phosphonobutyric acid: a new pharmacological tool for retina research. Science. 1981; 211:182–185. [PubMed: 6255566]

184. Smeraski CA, Sollars PJ, Ogilvie MD, Enquist LW, Pickard GE. Suprachiasmatic nucleus input to autonomic circuits identified by retrograde transsynaptic transport of pseudorabies virus from the eye. J Comp Neurol. 2004; 471:298–313. [PubMed: 14991563]

185. Sollars PJ, Smeraski CA, Kaufman JD, Ogilvie MD, Provencio I, Pickard GE. Melanopsin and non-melanopsin expressing retinal ganglion cells innervate the hypothalamic suprachiasmatic nucleus. Vis Neurosci. 2003; 20:601–610. [PubMed: 15088713]

186. Soucy E, Wang Y, Nirenberg S, Nathans J, Meister M. A novel signaling pathway from rod photoreceptors to ganglion cells in mammalian retina. Neuron. 1998; 21:481–493. [PubMed: 9768836]

187. Stevens RG. Circadian disruption and breast cancer: from melatonin to clock genes. Epidemiology. 2005; 16:254–258. [PubMed: 15703542]

188. Taddese A, Bean BP. Subthreshold sodium current from rapidly inactivating sodium channels drives spontaneous firing of tube-romammillary neurons. Neuron. 2002; 33:587–600. [PubMed: 11856532]

189. Takahashi JS, DeCoursey PJ, Bauman L, Menaker M. Spectral sensitivity of a novel photoreceptive system mediating entrainment of mammalian circadian rhythms. Nature. 1984; 308:186–188. [PubMed: 6700721]

190. Takahashi JS, Hong HK, Ko CH, McDearmon EL. The genetics of mammalian circadian order and disorder: implications for physiology and disease. Nat Rev Genet. 2008; 9:764–775. [PubMed: 18802415]

191. Tarttelin EE, Bellingham J, Bibb LC, Foster RG, Hankins MW, Gregory-Evans K, Gregory-Evans CY, Wells DJ, Lucas RJ. Expression of opsin genes early in ocular development of humans and mice. Exp Eye Res. 2003; 76:393–396. [PubMed: 12573668]

192. Terakita A. The opsins. Genome Biol. 2005; 6:213. [PubMed: 15774036]

193. Terakita A, Tsukamoto H, Koyanagi M, Sugahara M, Yamashita T, Shichida Y. Expression and comparative characterization of Gq-coupled invertebrate visual pigments and melanopsin. J Neurochem. 2008; 105:883–890. [PubMed: 18088357]

194. Terman M, Terman JS. Light therapy for seasonal and nonseasonal depression: efficacy, protocol, safety, and side effects. CNS Spectr. 2005; 10:647–663. [PubMed: 16041296]

195. Thapan K, Arendt J, Skene DJ. An action spectrum for melatonin suppression: evidence for a novel non-rod, non-cone photoreceptor system in humans. J Physiol. 2001; 535:261–267. [PubMed: 11507175]

196. Thompson CL, Blaner WS, Van Gelder RN, Lai K, Quadro L, Colantuoni V, Gottesman ME, Sancar A. Preservation of light signaling to the suprachiasmatic nucleus in vitamin A-deficient mice. Proc Natl Acad Sci USA. 2001; 98:11708–11713. [PubMed: 11562477]

197. Thompson S, Foster RG, Stone EM, Sheffield VC, Mrosovsky N. Classical and melanopsin photoreception in irradiance detection: negative masking of locomotor activity by light. Eur J Neurosci. 2008; 27:1973–1979. [PubMed: 18412618]

198. Tomonari S, Takagi A, Akamatsu S, Noji S, Ohuchi H. A non-canonical photopigment, melanopsin, is expressed in the differentiating ganglion, horizontal, and bipolar cells of the chicken retina. Dev Dyn. 2005; 234:783–790. [PubMed: 16217736]

199. Tomonari S, Takagi A, Noji S, Ohuchi H. Expression pattern of the melanopsin-like (*cOpn4m*) and VA opsin-like genes in the developing chicken retina and neural tissues. Gene Expr Patterns. 2007; 7:746–753. [PubMed: 17631423]

200. Torii M, Kojima D, Okano T, Nakamura A, Terakita A, Shichida Y, Wada A, Fukada Y. Two isoforms of chicken melanopsins show blue light sensitivity. FEBS Lett. 2007; 581:5327–5331. [PubMed: 17977531]

201. Tosini G, Aguzzi J, Bullock NM, Liu C, Kasamatsu M. Effect of photoreceptor degeneration on circadian photoreception and free-running period in the Royal College of Surgeons rat. Brain Res. 2007; 1148:76–82. [PubMed: 17382912]

202. Trejo LJ, Cicerone CM. Retinal sensitivity measured by the pupillary light reflex in RCS and albino rats. Vision Res. 1982; 22:1163–1171. [PubMed: 7147727]

203. Tsai JW, Hannibal J, Hagiwara G, Colas D, Ruppert E, Ruby NF, Heller HC, Franken P, Bourgin P. Melanopsin as a sleep modulator: circadian gating of the direct effects of light on sleep and

altered sleep homeostasis in *Opn4(−/−)* mice. PLoS Biol. 2009; 7:e1000125. [PubMed: 19513122]

204. Tu DC, Owens LA, Anderson L, Golczak M, Doyle SE, McCall M, Menaker M, Palczewski K, Van Gelder RN. Inner retinal photoreception independent of the visual retinoid cycle. Proc Natl Acad Sci USA. 2006; 103:10426–10431. [PubMed: 16788071]
205. Tu DC, Zhang D, Demas J, Slutsky EB, Provencio I, Holy TE, Van Gelder RN. Physiologic diversity and development of intrinsically photosensitive retinal ganglion cells. Neuron. 2005; 48:987–999. [PubMed: 16364902]
206. Van Gelder RN, Gibler TM, Tu D, Embry K, Selby CP, Thompson CL, Sancar A. Pleiotropic effects of cryptochromes 1 and 2 on free-running and light-entrained murine circadian rhythms. J Neurogenet. 2002; 16:181–203. [PubMed: 12696673]
207. Van Gelder RN, Wee R, Lee JA, Tu DC. Reduced pupillary light responses in mice lacking cryptochromes. Science. 2003; 299:222. [PubMed: 12522242]
208. Viney TJ, Balint K, Hillier D, Siegert S, Boldogkoi Z, Enquist LW, Meister M, Cepko CL, Roska B. Local retinal circuits of melanopsin-containing ganglion cells identified by transsynaptic viral tracing. Curr Biol. 2007; 17:981–988. [PubMed: 17524644]
209. Vize PD. Transcriptome analysis of the circadian regulatory network in the coral *Acropora millepora*. Biol Bull. 2009; 216:131–137. [PubMed: 19366924]
210. Vugler AA, Redgrave P, Hewson-Stoate NJ, Greenwood J, Coffey PJ. Constant illumination causes spatially discrete dopamine depletion in the normal and degenerate retina. J Chem Neuroanat. 2007; 33:9–22. [PubMed: 17223011]
211. Vugler AA, Redgrave P, Semo M, Lawrence J, Greenwood J, Coffey PJ. Dopamine neurones form a discrete plexus with melanopsin cells in normal and degenerating retina. Exp Neurol. 2007; 205:26–35. [PubMed: 17362933]
212. Walker MT, Brown RL, Cronin TW, Robinson PR. Photochemistry of retinal chromophore in mouse melanopsin. Proc Natl Acad Sci USA. 2008; 105:8861–8865. [PubMed: 18579788]
213. Walker MT, Robinson PR. Spectral analysis of endogenous mouse melanopsin. Invest Ophthalmol Visual Sci. 2007; 48:E-Abstract 4642.
214. Wan J, Zheng H, Hu BY, Xiao HL, She ZJ, Chen ZL, Zhou GM. Acute photoreceptor degeneration down-regulates melanopsin expression in adult rat retina. Neurosci Lett. 2006; 400:48–52. [PubMed: 16580133]
215. Wang HZ, Lu QJ, Wang NL, Liu H, Zhang L, Zhan GL. Loss of melanopsin-containing retinal ganglion cells in a rat glaucoma model. Chin Med J. 2008; 121:1015–1019. [PubMed: 18706250]
216. Wang JS, Estevez ME, Cornwall MC, Kefalov VJ. Intra-retinal visual cycle required for rapid and complete cone dark adaptation. Nat Neurosci. 2009; 12:295–302. [PubMed: 19182795]
217. Wang JS, Kefalov VJ. An alternative pathway mediates the mouse and human cone visual cycle. Curr Biol. 2009; 19:1665–1669. [PubMed: 19781940]
218. Wark B, Lundstrom BN, Fairhall A. Sensory adaptation. Curr Opin Neurobiol. 2007; 17:423–429. [PubMed: 17714934]
219. Warren EJ, Allen CN, Brown RL, Robinson DW. Intrinsic light responses of retinal ganglion cells projecting to the circadian system. Eur J Neurosci. 2003; 17:1727–1735. [PubMed: 12752771]
220. Warren EJ, Allen CN, Brown RL, Robinson DW. The light-activated signaling pathway in SCN-projecting rat retinal ganglion cells. Eur J Neurosci. 2006; 23:2477–2487. [PubMed: 16706854]
221. Wassle H, Chun MH. Dopaminergic and indoleamine-accumulating amacrine cells express GABA-like immunoreactivity in the cat retina. J Neurosci. 1988; 8:3383–3394. [PubMed: 2902202]
222. Weaver DR, Reppert SM. Definition of the developmental transition from dopaminergic to photic regulation of c-*fos* gene expression in the rat suprachiasmatic nucleus. Brain Res. 1995; 33:136–148.
223. Weng S, Berson DM. Ganglion-cell photoreceptors are driven by the most sensitive rod pathway and by cones. Invest Ophthalmol Vis Sci. 2009; 50:E-Abstract 2556.
224. Weng S, Wong KY, Berson DM. Circadian modulation of melanopsin-driven light response in rat ganglion-cell photoreceptors. J Biol Rhythms. 2009; 24:391–402. [PubMed: 19755584]

225. Werblin FS, Dowling JE. Organization of the retina of the mud-puppy, *Necturus maculosus*. II. Intracellular recording. J Neurophysiol. 1969; 32:339–355. [PubMed: 4306897]

226. Witkovsky P. Dopamine and retinal function. Doc Ophthalmol. 2004; 108:17–40. [PubMed: 15104164]

227. Wong KY, Dunn FA, Berson DM. Photoreceptor adaptation in intrinsically photosensitive retinal ganglion cells. Neuron. 2005; 48:1001–1010. [PubMed: 16364903]

228. Wong KY, Dunn FA, Graham DM, Berson DM. Synaptic influences on rat ganglion-cell photoreceptors. J Physiol. 2007; 582:279–296. [PubMed: 17510182]

229. Yau KW, Hardie RC. Phototransduction motifs and variations. Cell. 2009; 139:246–264. [PubMed: 19837030]

230. Yoshimura T, Ebihara S. Spectral sensitivity of photoreceptors mediating phase-shifts of circadian rhythms in retinally degenerate CBA/J (*rd*/*rd*) and normal CBA/N (+/+) mice. J Comp Physiol A Sens Neural Behav Physiol. 1996; 178:797–802.

231. Young RS, Kimura E. Pupillary correlates of light-evoked melanopsin activity in humans. Vision Res. 2008; 48:862–871. [PubMed: 18262584]

232. Zaidi FH, Hull JT, Peirson SN, Wulff K, Aeschbach D, Gooley JJ, Brainard GC, Gregory-Evans K, Rizzo JF 3rd, Czeisler CA, Foster RG, Moseley MJ, Lockley SW. Short-wavelength light sensitivity of circadian, pupillary, and visual awareness in humans lacking an outer retina. Curr Biol. 2007; 17:2122–2128. [PubMed: 18082405]

233. Zawilska JB, Skene DJ, Arendt J. Physiology and pharmacology of melatonin in relation to biological rhythms. Pharmacol Rep. 2009; 61:383–410. [PubMed: 19605939]

234. Zhang DQ, Wong KY, Sollars PJ, Berson DM, Pickard GE, McMahon DG. Intraretinal signaling by ganglion cell photoreceptors to dopaminergic amacrine neurons. Proc Natl Acad Sci USA. 2008; 105:14181–14186. [PubMed: 18779590]

235. Zhang DQ, Zhou TR, McMahon DG. Functional heterogeneity of retinal dopaminergic neurons underlying their multiple roles in vision. J Neurosci. 2007; 27:692–699. [PubMed: 17234601]

236. Zhu Y, Tu DC, Denner D, Shane T, Fitzgerald CM, Van Gelder RN. Melanopsin-dependent persistence and photopotentiation of murine pupillary light responses. Invest Ophthalmol Vis Sci. 2007; 48:1268–1275. [PubMed: 17325172]

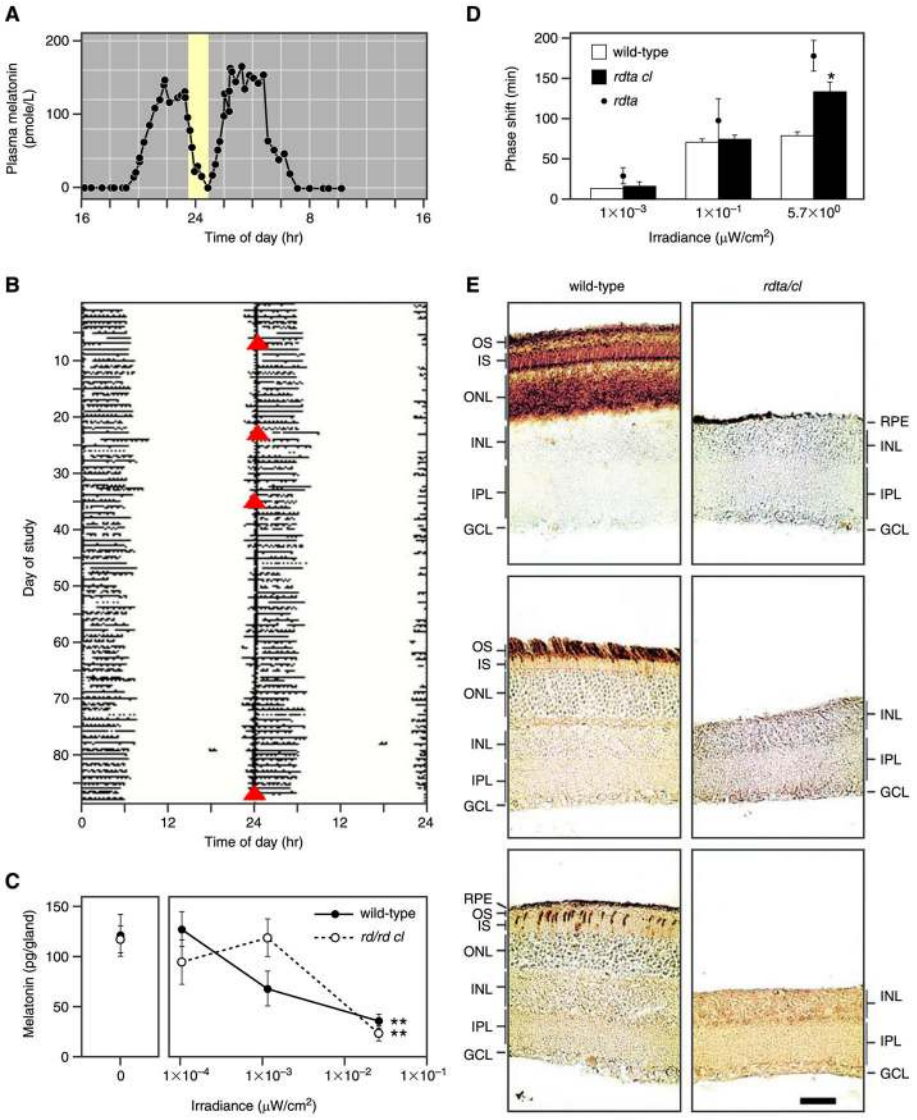

FIG. 1.

Photoreception without rods and cones. *A*: suppression of plasma melatonin by light (lighter region) in a patient who was blind from Leber's congenital amaurosis and lacked a detectable electroretinogram. *B*: the sleep-wake pattern of the blind patient in *A*. Solid horizontal lines represent periods of sleep, and open triangles (red) indicate times of peak plasma melatonin level (a marker of the patient's endogenous circadian period). This patient's activity patterns were entrained to the environmental 24-h cycle. [*A* and *B* modified from Czeisler et al. (34).] *C*: suppression of melatonin synthesis in wild-type and rodless/coneless mice by light of different irradiances. [Modified from Lucas et al. (115).] *D*: shift of circadian phase in wild-type, rodless/coneless (*rdta/cl*), and rodless (*rdta*) mice by light of different irradiances. *E*: retinal cross-sections of wild-type and rodless/coneless (*rdta/cl*) mice stained with antibodies recognizing rod pigment *(top)*, rod and green cone pigments *(middle)*, and ultraviolet cone pigment *(bottom)* to demonstrate that no outer retinal photoreceptors are detectable in rodless/coneless mice. The same was observed for retinas of

rd/rd cl mice used for *C*. OS, outer segments; IS, inner segments; ONL, outer nuclear layer; INL, inner nuclear layer; IPL, inner plexiform layer; GCL, ganglion cell layer; RPE, retinal pigment epithelium. Scale bar is 40 μm. [*D* and *E* modified from Freedman et al. (52).]

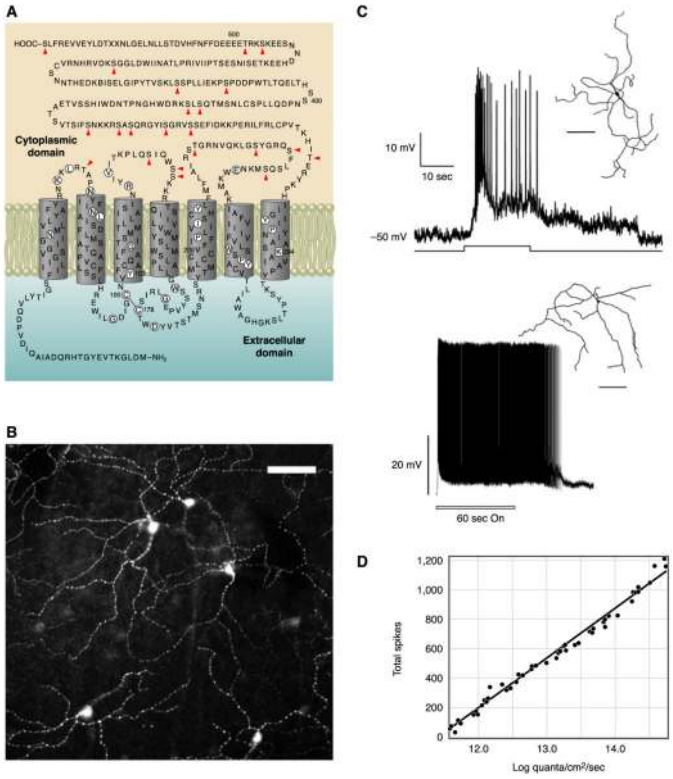

FIG. 2.

Intrinsic photosensitivity of retinal ganglion cells expressing melanopsin. *A*: predicted secondary structure of melanopsin cloned from *Xenopus laevis*. [Modified from Provencio et al. (155).] *B*: immunostaining for melanopsin in a flattened mouse retina revealing a population of retinal ganglion cells with extensive dendritic arbors. Scale bar is 100 μm. [Modified from Provencio et al. (157).] *C, top*: an ipRGC in the rat identified by retrograde-labeling from the suprachiasmatic nucleus (SCN) and studied with patch-clamp electrophysiological recording. Even with pharmacological block of synaptic transmission, this cell depolarized to light and fired action potentials. *Inset* shows camera lucida drawing of the recorded cell. [Modified from Berson et al. (17).] *Bottom*: microelectrode recording from a macaque ipRGC also showing intrinsic photosensitivity. *Inset* shows tracing of a macaque melanopsin-expressing retinal ganglion cell. Scale bars in *top* and *bottom* are 100 and 200 μm, respectively. *D*: total number of spikes elicited by a 10-s light stimulus rising monotonically with light intensity for a macaque ipRGC recorded with synaptic transmission blocked. [*C* and *D* modified from Dacey et al. (35).]

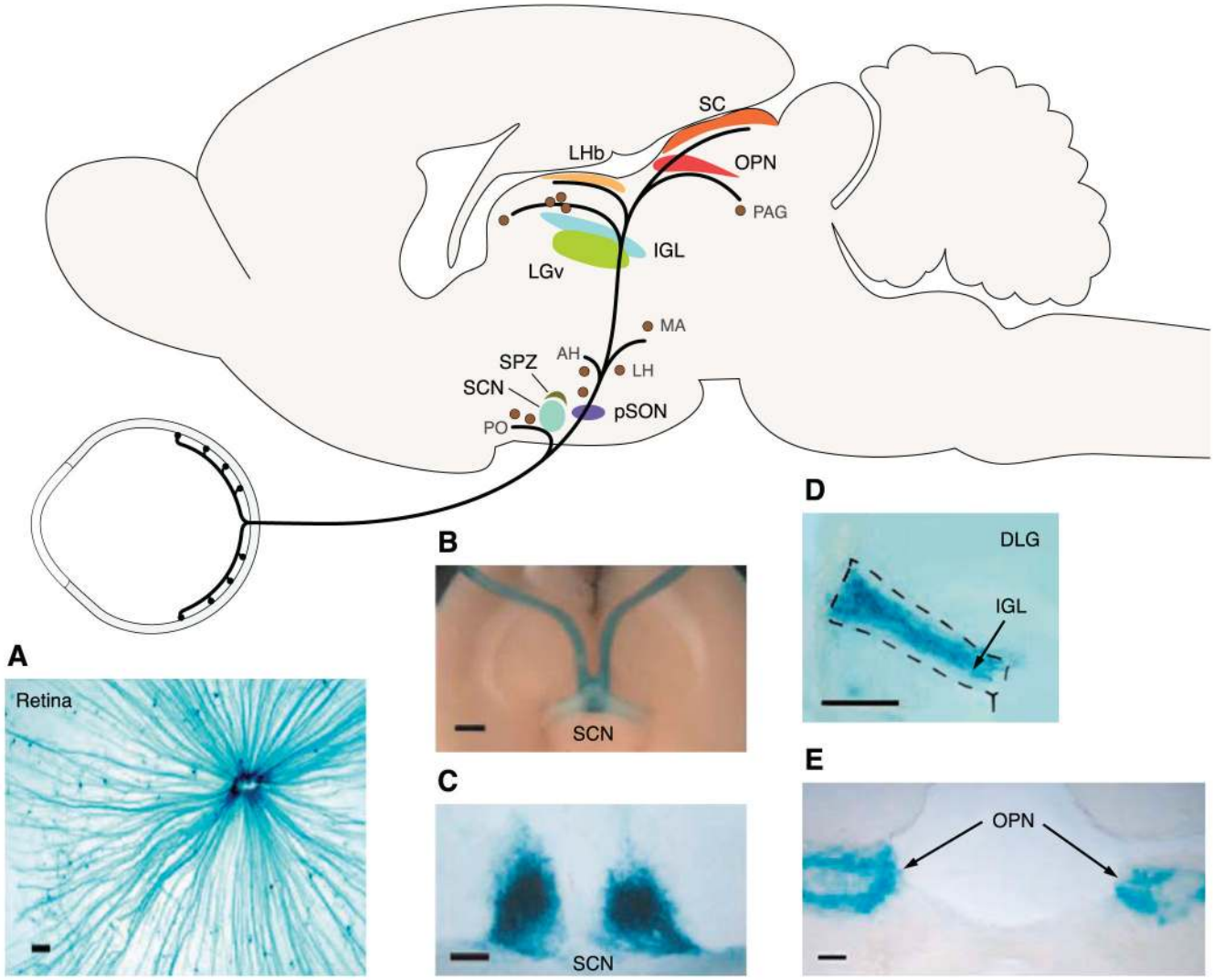

FIG. 3.

Brain targets of ipRGCs. A schematic of the mouse brain in sagittal view showing a sampling of regions innervated by ipRGCs. [Modified from Hattar et al. (87).] PO, preoptic area; SCN, suprachiasmatic nucleus; SPZ, subparaventricular zone; pSON, peri-supraoptic nucleus; AH, anterior hypothalamic nucleus; LH, lateral hypothalamus; MA, medial amygdaloid nucleus; LGv, ventral lateral geniculate nucleus; IGL, intergeniculate leaflet; BST, bed nucleus of the stria terminalis; LGd, dorsal lateral geniculate nucleus; LHb, lateral habenula; SC, superior colliculus; OPN, olivary pretectal nucleus; PAG, periaqueductal gray. *A*: flat-mount retina of a mouse with the *tau-lacZ* marker gene targeted into the melanopsin gene locus (*opn4*$^{+/-}$ *tauLacZ*$^{+/-}$). Blue color shows X-gal staining of the β-galactosidase activity coded by *tau-lacZ* in the ipRGCs. IpRGC axons can be seen coursing to the optic disc. Scale bar is 100 μm. [Modified from Hattar et al. (89).] *B*: ventral view of the *opn4*$^{+/-}$ *tauLacZ*$^{+/-}$ brain showing ipRGC axons running in the optic nerve and innervating the suprachiasmatic nuclei (SCN). Scale bar is 1 mm. *C*: coronal section of the *opn4*$^{+/-}$ *tauLacZ*$^{+/-}$ mouse brain showing dense innervation of the SCN. Scale bar is 100

μm. *D*: prominent innervation of the intergeniculate leaflet (IGL) by ipRGC axons. Coronal section, scale bar is 100 μm. DLG, dorsal lateral geniculate nucleus. [*B–D* modified from Hattar et al. (88).] *E*: olivary pretectal nucleus (OPN) is a major target of ipRGCs. Coronal section, scale bar is 100 μm. [Modified from Lucas et al. (116).]

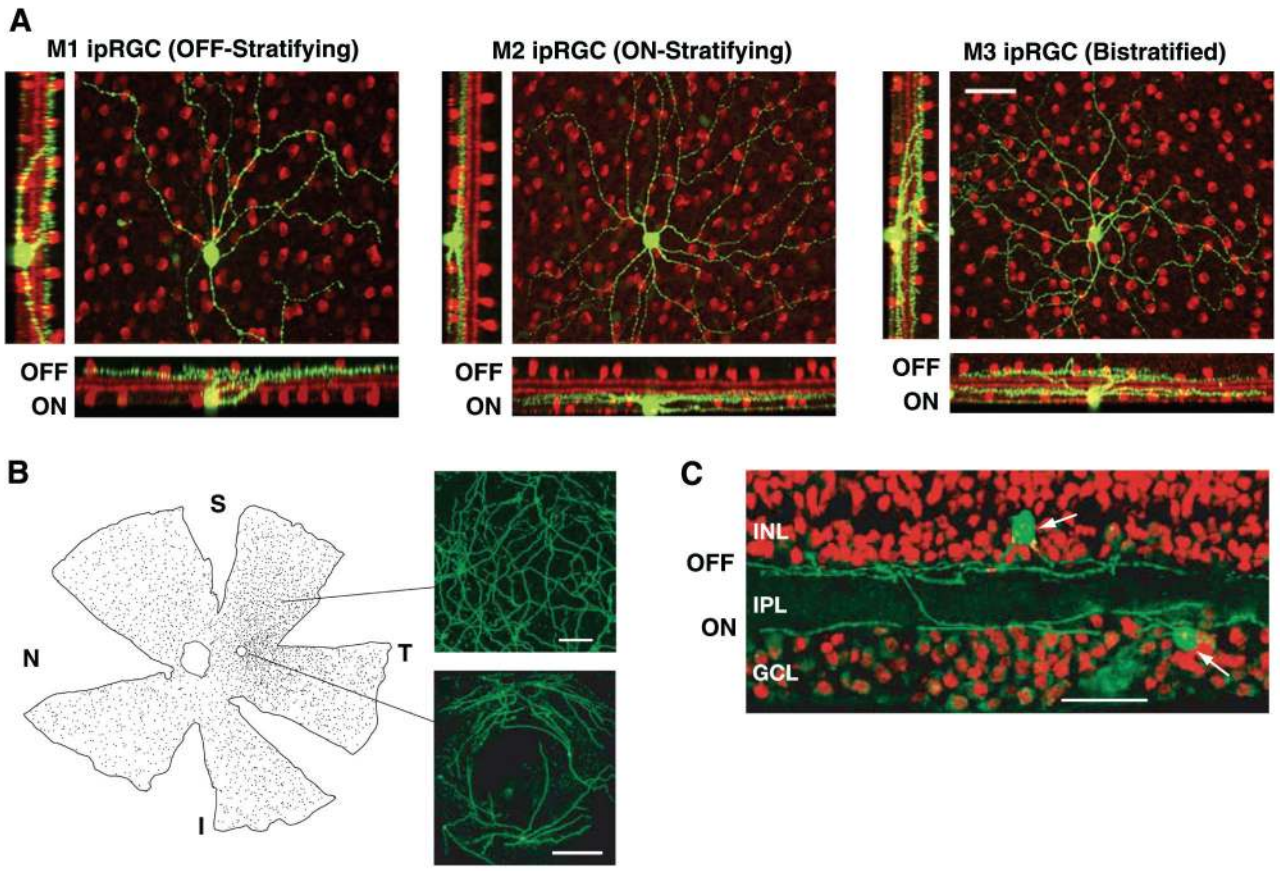

FIG. 4.

Morphological diversity and distribution of ipRGCs. *A*: stacked confocal micrographs demonstrating three morphological subclasses of ipRGCs in mouse. IpRGCs were filled with neurobiotin (green) and the retinas processed for choline acetyltransferase (red) to visualize a population of amacrine cells as anatomical markers. Scale bar is 50 μm. [Modified from Schmidt et al. (174).] *B, left*: distribution of melanopsin-expressing retinal ganglion cells (dots) in the macaque retina. Superior (S), nasal (N), temporal (T), and inferior (I) directions are indicated. Small open circle is the fovea. *Right*: higher power views of melanopsin cells in the peripheral retina (*top*, scale bar is 100 μm) and near the fovea (*bottom*, scale bar is 200 μm). Note that melanopsin-cell dendrites and somata encircle but do not enter the fovea. *C*: stacked confocal images of vertical sections through the macaque retina immunostained with melanopsin (green) and counterstained with propidium iodide (red). Note a melanopsin cell displaced to the INL and stratifying its dendrites in the OFF sublamina of the IPL, and another in the GCL and stratifying in the ON sublamina of the IPL (arrows). Scale bar is 50 μm. [*B* and *C* modified from Dacey et al. (35).]

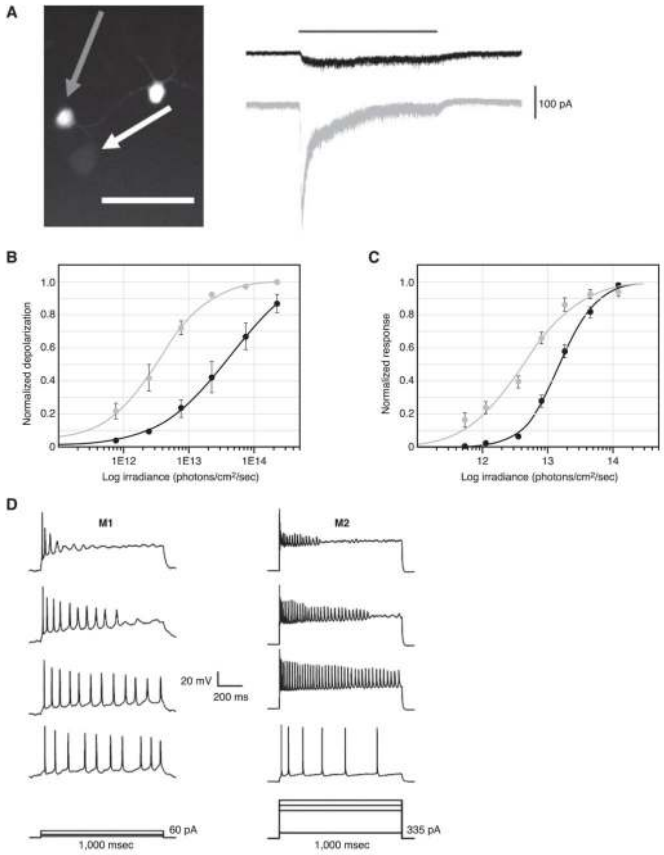

FIG. 5.

Physiological diversity of ipRGCs. *A*: simultaneous voltage-clamp recordings from an M1 (gray arrow) and an M2 (white arrow) ipRGC in the flat-mount retina, identified by reporter-gene expression in a melanopsin BAC-transgenic mouse. Synaptic transmission is blocked pharmacologically. The M1 cell shows a much larger intrinsic photocurrent (gray trace on *right*) than does the M2 cell (black trace) in response to the same light stimulus. Scale bar is 50 μm. *B*: light-evoked depolarization (recorded in current clamp) in the two ipRGC subtypes as a function of light intensity. M1 cells (gray curve) are roughly 10-fold more sensitive than M2 cells (black curve) at 32–34°C. [*A* and *B* modified from Schmidt and Kofuji (173).] *C*: an early demonstration of physiological diversity of ipRGCs using multielectrode-array recording from retinas of rod/cone-degenerated mice. The total number of light-induced spikes is plotted for two populations of cells in the adult mouse discriminated by cluster analysis at 35°C. [Modified from Tu et al. (205).] *D:* M1 and M2 ipRGCs also differ in intrinsic membrane properties, with the former firing spikes at a lower rate and being more prone to depolarization block. Whole cell, current-clamp recordings from ipRGCs in flat-mount retinas with synaptic transmission blocked are shown at room temperature. [Modified from Schmidt and Kofuji (173).].

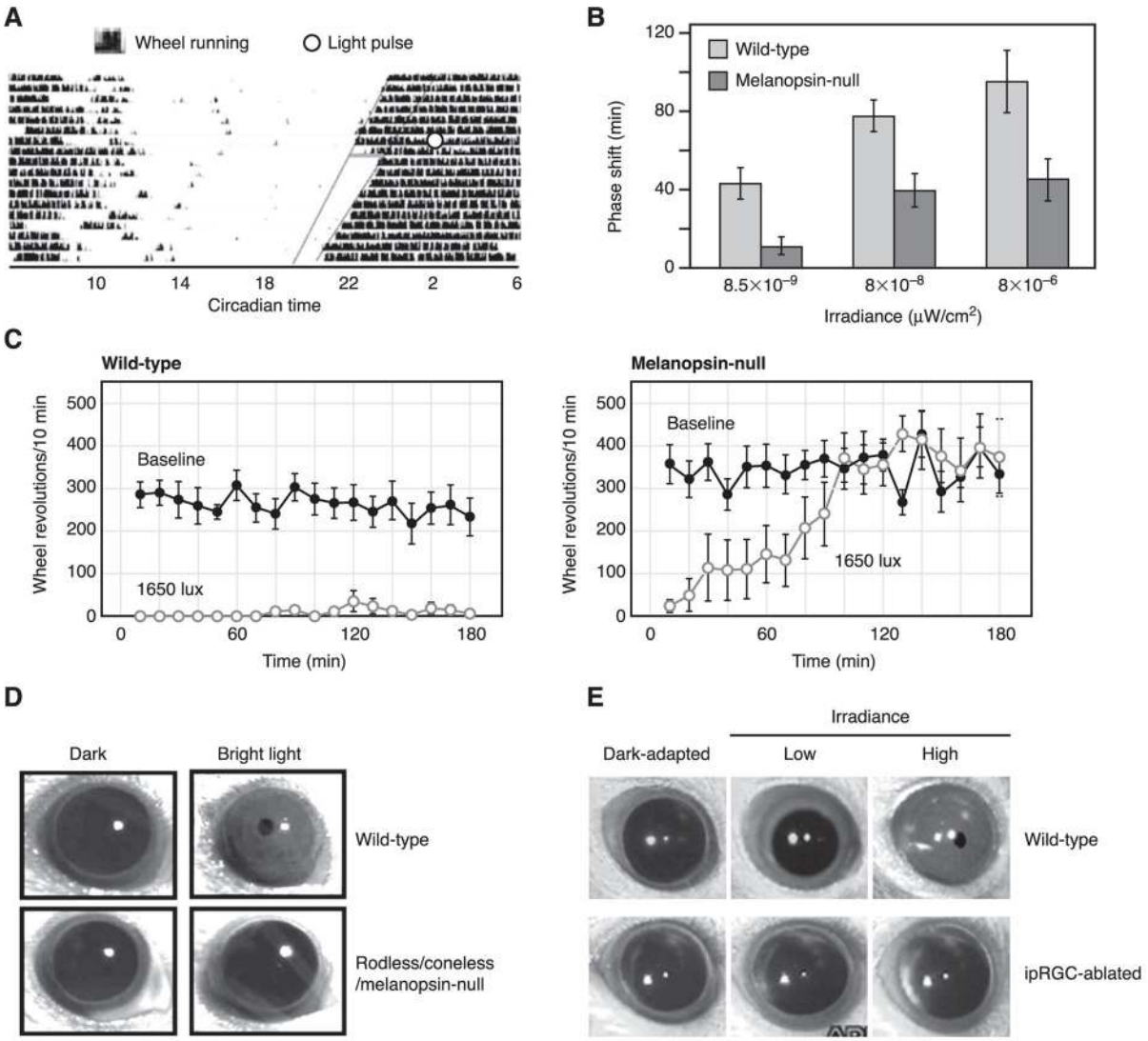

FIG. 6.

Whole-animal photic functions involving ipRGCs. *A*: actogram showing circadian-phase shifting of a wild-type mouse in complete darkness. Dark vertical blips represent wheel-running activity, plotted on a double 24-h time cycle. The endogenous circadian period of this mouse is slightly under 24 h, producing an earlier initiation of activity on each successive day. A 15-min pulse of light given soon after the initiation of activity (open circle) results in a phase shift, with activity beginning with a delay on the next day. *B*: the extent of phase-shifting for wild-type and melanopsin-null (*opn4*$^{-/-}$) mice, with light of different intensities. [*A* and *B* modified from Panda et al. (145).] *C*: negative masking (arrest of locomotor activity) for wild-type (*left*) and melanopsin-null (*right*) mice. Melanopsin-null mice can initiate, but not sustain, negative masking by light. Solid circles represent wheel-running activity in darkness. Open circles represent wheel-running activity in light, switched on at *time 0*. [Modified from Mrosovsky and Hattar (133).] *D*: pupillary light reflex (PLR) of wild-type mouse and mouse lacking rods/cones and melanopsin ("triple-null" mouse). Triple-null mouse shows virtually no PLR to a light that drives a maximum pupil

constriction in the wild-type mouse (*top*). [Modified from Hattar et al. (89).] *E*: PLR of wild-type mouse and mouse with ipRGCs largely genetically ablated by targeted, conditional expression of diphtheria-toxin receptor followed by administration of diphtheria toxin. In mice with intact, functioning rods and cones, conditional ablation of ipRGCs eliminated the PLR. [Modified from Hatori et al. (85).].

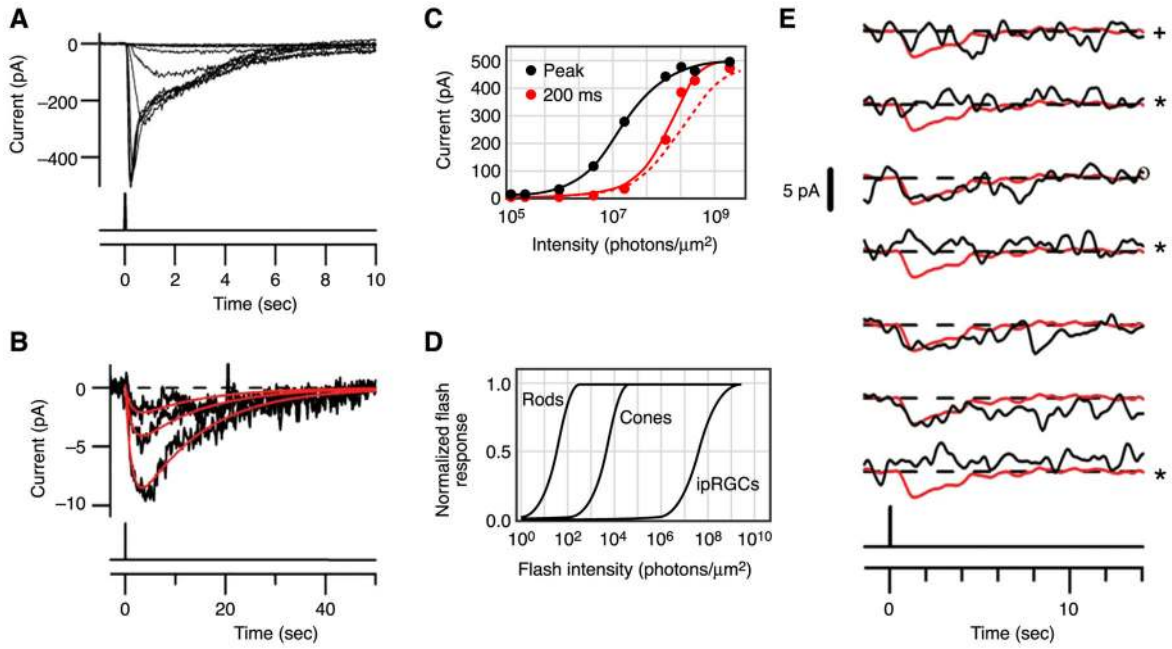

FIG. 7.

Flash response and absolute sensitivity of ipRGCs. *A*: responses of an ipRGC in the flat-mount retina to diffuse 50-ms flashes at different intensities. Stimulus timing is shown below. *B*: three smallest responses from *A*, elicited by successive approximate doublings of flash intensity, on expanded ordinate and longer time base, to demonstrate linearity. Responses fit with the same convolution of two single-exponential decays but scaled by the relative flash intensities (red). *C*: intensity-response relationships plotted from *A*. Black circles, peak response-intensity relationship fit with Michaelis equation; red circles, instantaneous intensity-response relationship at 200 ms from flash onset, fit with a saturating exponential function. Dashed curve is a Michaelis fit aligned for comparison with saturating-exponential fit. *D*: comparison of flash intensity-response relations for rods, cones, and ipRGCs. Rod and cone relations are saturating exponentials (not very different from Michaelis in shape or, for rods and cones, the half-saturating flash intensity), and ipRGC relation is Michaelis. *E*: partial series of responses of an in situ ipRGC to repeated identical flashes, mostly too dim to elicit a response, at 35°C. The unitary response, by fluctuation analysis, was 2.3 pA. Red traces are identical and represent the expected profile of the unitary response (a brighter flash within the linear range of the cell, scaled to 2.3 pA). Apparent failures (marked by *) and an ambiguous trial (marked by +) were judged according to several detection algorithms. [*A*–*E* modified from Do et al. (39).]

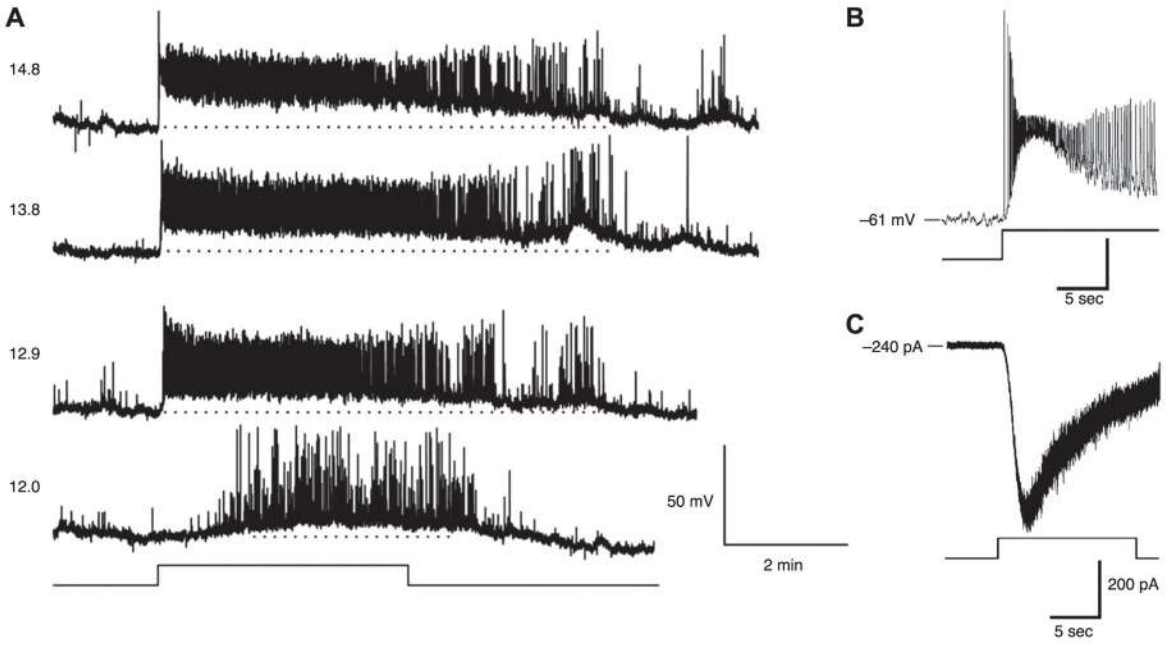

FIG. 8.

Step response and adaptation of ipRGCs. *A*: an ipRGC recorded in the flat-mount rat retina under current clamp, showing sustained firing during long steps of light. Numbers to the *left* of each trace represent the log irradiance (500 nm photons·cm^{-2}·s^{-1}). [Modified from Berson et al. (17).] *B*: adaptation to light in spike-firing by ipRGCs in current clamp. *C*: adaptation of intrinsic photocurrent, recorded in voltage clamp, to light. [*B* and *C* modified from Wong et al. (227).] All recordings with synaptic transmission blocked and at room temperature.

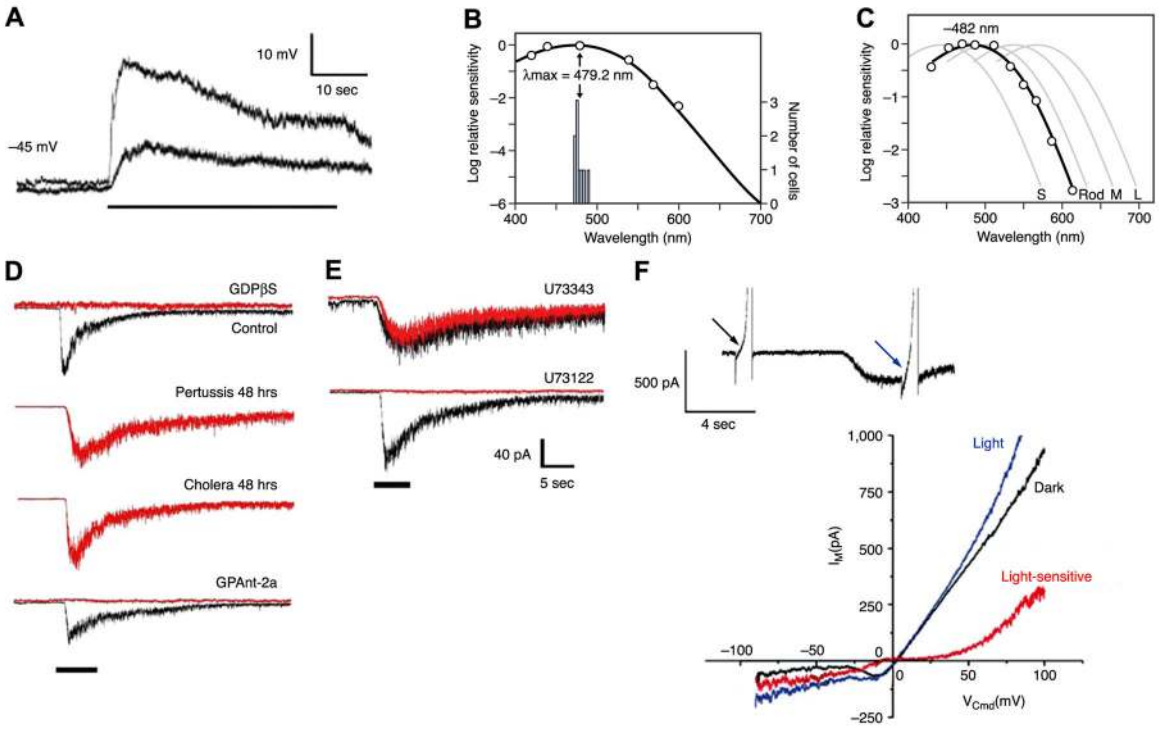

FIG. 9.

Melanopsin phototransduction. *A*: heterologous expression of mouse melanopsin conferring photosensitivity to a HEK293 cell. Traces show voltage responses to two light intensities (stimulus marked by horizontal bar below the traces). *B*: spectral sensitivity of light response of HEK293 cells expressing melanopsin heterologously. Curve is opsin-based pigment nomogram with λ_{max} = ~480 nm, similar to that of ipRGCs. [*A* and *B* modified from Qiu et al. (161).] *C*: spectral sensitivity of macaque ipRGC with nomogram fit, together with those (faint curves) of macaque rods as well as macaque short- (S), medium- (M), and long-wavelength (L) cones. [Modified from Dacey et al. (35).] *D*: block of intrinsic photosensitivity of cultured rat ipRGCs by GDP*β*S (general G protein blocker) and by GPAnt-2 (G_q subfamily blocker) but not following prolonged exposure to pertussis and cholera toxins (which affect G_i and G_s subfamilies, respectively). *E*: block of intrinsic photosensitivity of cultured rat ipRGCs by U73122 (phospholipase C blocker) but not by its inactive analog. [*D* and *E* modified from Graham et al. (65).] *F*: current-voltage relation of the intrinsic photocurrent. The membrane currents of an ipRGC elicited by voltage ramps delivered in darkness (black) and light (blue). Difference gives the light-sensitive current (red). [Modified from Warren et al. (219).]

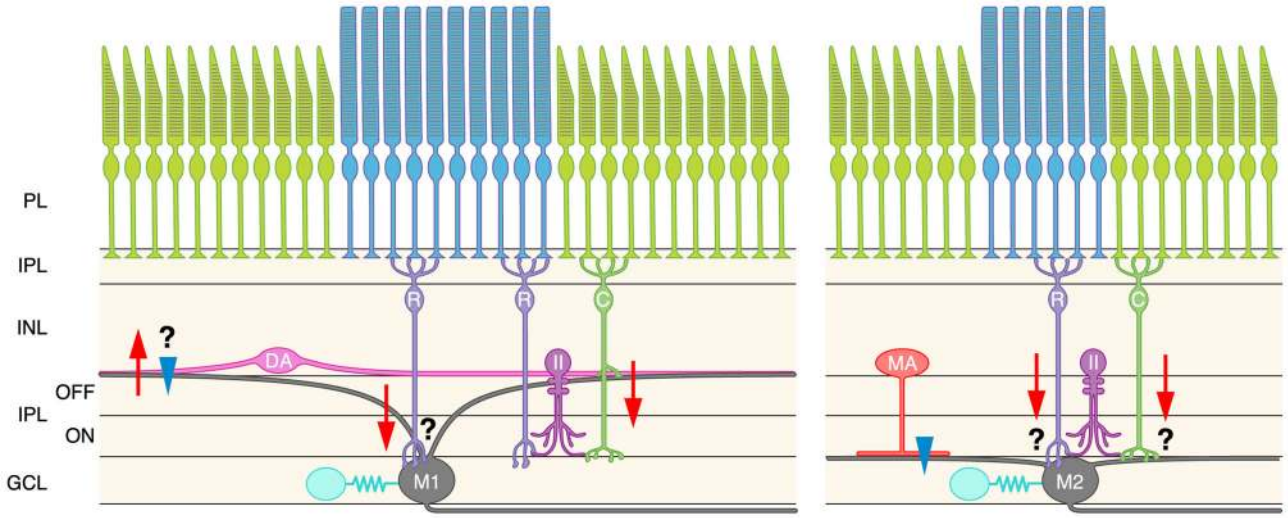

FIG. 10.

Schematic of ipRGCs and retinal circuitry. A schematic of the retinal cross-section, illustrating the reported circuitry of M1 (*left*) and M2 (*right*) ipRGCs. Downward-pointing arrows indicate transmission to ipRGCs, and upward-pointing arrows indicate transmission from ipRGCs. Red arrows indicate excitation, and blue arrowheads indicate inhibition. Question marks indicate connections/interactions awaiting confirmation from electrophysiology. M1, M1 ipRGC; M2, M2 ipRGC; R, rod bipolar cell; C, cone bipolar cell; II, AII amacrine cell; MA, monostratified amacrine cell; DA, dopaminergic amacrine cell; PL. photoreceptor layer; IPL, inner plexiform layer; INL, inner nuclear layer; GCL, ganglion cell layer. IpRGCs are also coupled electrically to cells in the GCL (blue cells). The retinal circuitry of M3 cells has not been reported and thus is not illustrated here.

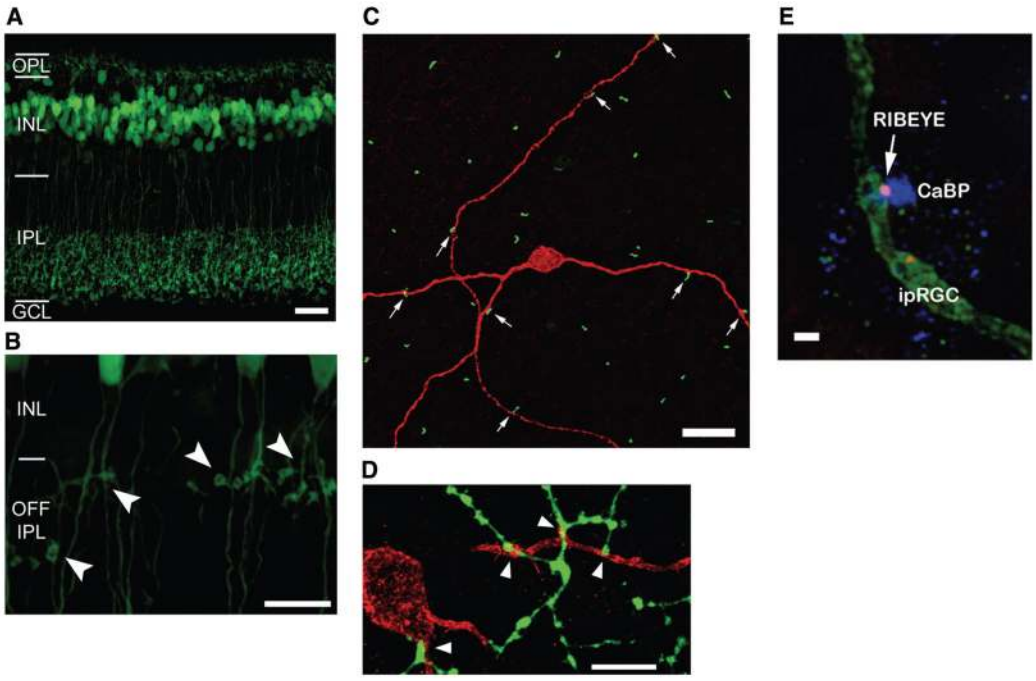

FIG. 11.

ON synapses in the OFF sublamina to ipRGCs. *A*: vertical section through a mouse retina expressing GFP under control of the mGluR6 promoter, active in ON cone bipolar cells. Scale bar is 20 μm. *B*: high-power view of section in *A* to show axonal swellings, which are en passant synapses, and lateral extensions from the axons terminating in swellings, which are ectopic synapses. Scale bar is 10 μm. [*A* and *B* modified from Dumitrescu et al. (43).] *C*: melanopsin immunostaining of a flat-mounted rabbit retina (red). Descending axons of calbindin-expressing bipolar cells (green) forming ectopic, en passant synapses on ipRGC dendrites in the OFF sublamina of the IPL. Scale bar is 20 μm. *D*: axon terminals of calbindin-expressing bipolar cells in rabbit (green) contacting ipRGC dendrites in the ON sublamina of the IPL. Scale bar is 10 μm. *E*: synaptic ribbons (positive for RIBEYE-immunostaining) colocalized with junctions between calbindin-positive axons (blue) and ipRGC dendrites (green). Scale bar is 1 μm. [*C*–*E* modified from Hoshi et al. (94).]

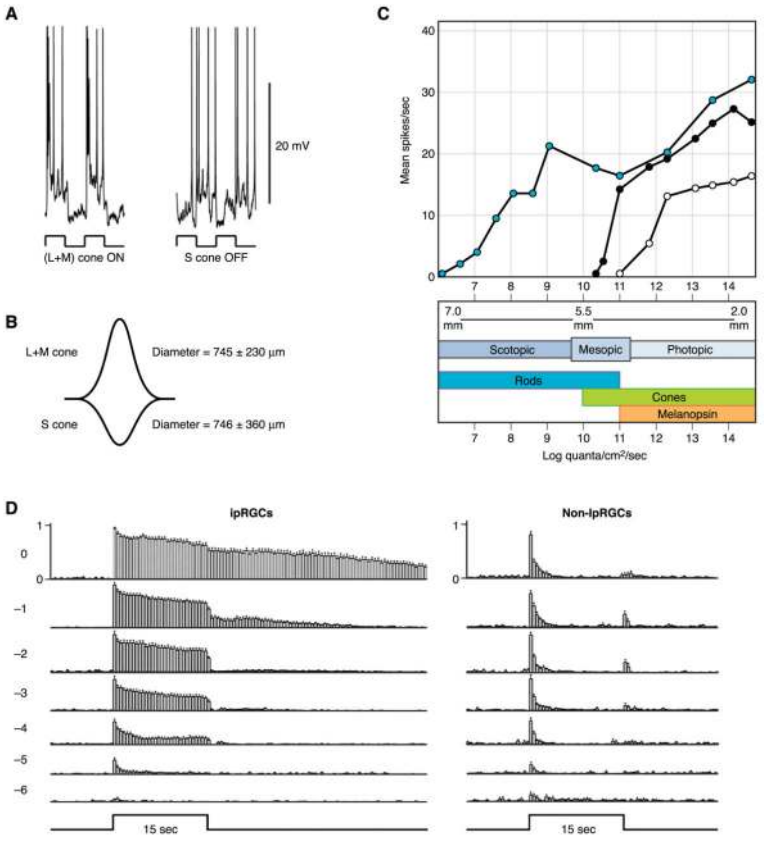

FIG. 12.

Synaptic drive to ipRGCs. *A*: macaque ipRGCs driven at light onset by long- and medium-wavelength cone signals, and at light offset by short-wavelength cone signals. *B*: receptive fields of ON and OFF responses are virtually coextensive and match the dendritic fields of the ipRGCs. Shown are Gaussian fits to the receptive fields. *C*: response of a macaque ipRGC to a 470-nm light step as a function of retinal illumination for 3 stimulus conditions: dark-adapted (blue circles), light-adapted (black circles), and light-adapted with synaptic block (open circles). Boxed area below plot shows melanopsin-associated, rod and cone response ranges in relation to scotopic, mesopic, and photopic ranges of human vision and pupil diameter. [*A–C* modified from Dacey et al. (35).] *D*: normalized, population spike rates of ipRGCs and conventional RGCs recorded by multielectrode array, with synaptic transmission intact. Signaling by ipRGCs is sustained, even at light intensities that are too low to drive intrinsic photosensitivity, suggesting that synaptic input to these neurons is also specialized for long-duration signaling. Numbers at left are log attenuations of the broadband tungsten-halogen light stimulus (unattenuated stimulus sampled at 480 nm, 2.3×10^{13} photons·cm^{-2}·s^{-1}). [Modified from Wong et al. (228).]

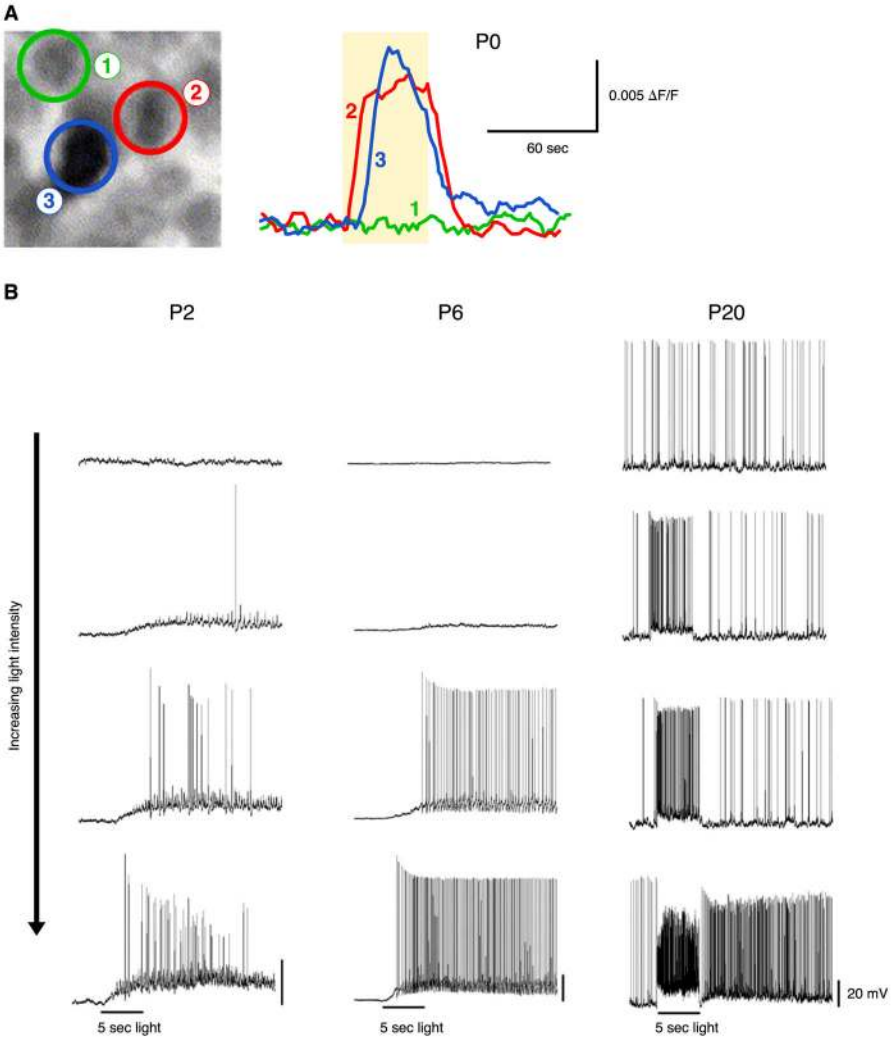

FIG. 13.

IpRGCs during development. *A*: calcium imaging of a retina taken from wild-type mouse at birth. Two of three cells studied in this field of view (*left*) showed a light-driven rise in calcium (*right*). Timing of the light stimulus shown by shaded region. [Modified from Sekaran et al. (178).] *B*: increase in photosensitivity of ipRGCs with age. Whole cell, current-clamp recordings from mouse ipRGCs in the flat-mount retina with synaptic transmission intact. Responses to four different light intensities are shown for three developmental times. [Modified from Schmidt et al. (174).]

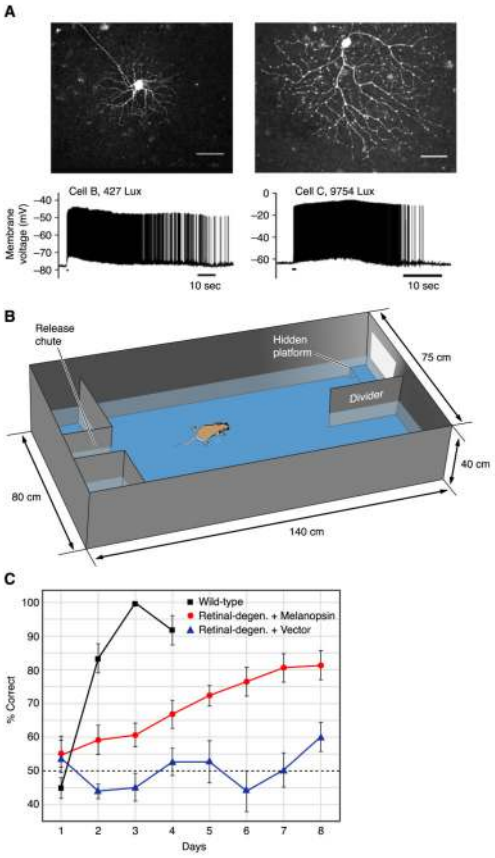

FIG. 14.

Potential clinical relevance of ipRGCs. *A*: conventional RGCs in rod/cone-degenerated mice, driven to express melanopsin by viral transduction. Whole cell current-clamp recording in flat-mount retina to study their physiology (at 32–35°C) and Lucifer Yellow injection to study their morphology. Light responses from two cells consisting of a long-lasting depolarization and action-potential firing are shown (stimulus timing and duration indicated by a short black bar beneath the recorded trace). Conventional RGCs expressing melanopsin responded to light even in rod/cone-degenerate retina and under pharmacological block of synaptic transmission. Scale bars are 50 μm. *B*: visual discrimination task. Mice swam down a water-filled alley toward an illuminated or dark compartment, with the rewarded stimulus being paired with the location of a submerged platform. *C*: melanopsin-transduced (open circles) mice outperforming control-transduced (triangles) rod/cone-degenerated mice in the visual detection task over an 8-day trial. [*A–C* modified from Lin et al. (111).]

TABLE 1

Brain targets of ipRGCs

IpRGC Target	Target Function	IpRGC Innervation
	Primary targets	
Suprachiasmatic nucleus	Master regulation of circadian rhythms	Dominant
Intergeniculate leaflet	Integration of photic and nonphotic circadian cues	Major
Olivary pretectal nucleus	Pupillary constriction	Major
Posterior thalamic nucleus, dorsal border (132)	Nociception (132)	Major (132)
Lateral habenula	Integration of limbic, motor, and circadian systems	Undetermined
	Secondary targets	
Dorsal lateral geniculate nucleus	Image-forming vision	Minor
Lateral hypothalamus	Energy homeostasis	Minor
Lateral posterior thalamic nucleus	Higher-order processing of thalamic, cortical, and visual signals	Moderate
Posterior limitans thalamic nucleus	Detection of rapid illumination changes for nonimage vision	Moderate
Superior colliculus	Integration of multiple modalities for gaze control	Minor
Ventral lateral geniculate nucleus	Visuomotor function	Minor
Ventral subparaventricular zone	Circadian and direct regulation of locomotion and sleep	Minor
Ventrolateral preoptic nucleus	Promotion of sleep	Minor

Selected brain regions innervated by intrinsically photosensitive retinal ganglion cells (ipRGCs) are listed with their general function (for a more comprehensive survey, see Refs. 63 and 87). Targets receiving dense innervations by ipRGC fibers are grouped at the top of the table, and others receiving weaker innervations are listed below in alphabetical order. IpRGC innervation refers to the density of ipRGC afferents relative to that of conventional RGCs. IpRGC innervation is predominantly contralateral for all regions except the SCN, which is largely bilateral. This list is not exhaustive. It is also likely to concern mostly the M1 ipRGCs, and other ipRGC subtypes may have different projections (see text). [Modified and updated from Fu et al. (54).]